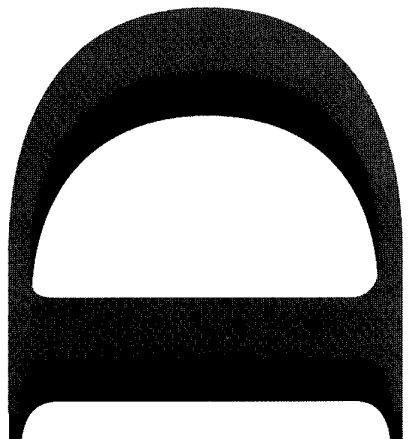
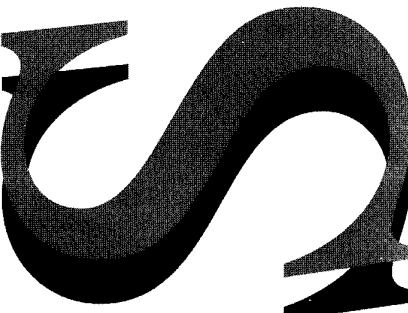
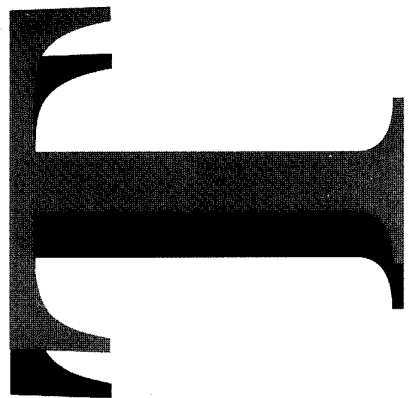


AR-009-476

DSTO-RR-0068



Acoustical Properties of the  
MOD Salisbury Test Tank and  
Techniques for Measurements

A.D. Jones and S.A. Hoefs

---

APPROVED FOR PUBLIC RELEASE

© Commonwealth of Australia

# Acoustical Properties of the MOD Salisbury Test Tank and Techniques for Measurements

*A. D. Jones and S. A. Hoefs*

**Maritime Operations Division  
Aeronautical and Maritime Research Laboratory**

DSTO-RR-0068

## ABSTRACT

The acoustical properties of the MOD test tank at DSTO Salisbury were determined, so that the limitations on its use for precise acoustical measurements might be known. The tank properties were measured according to the characterisation usually applied to air-filled reverberant chambers. The measurement of these properties is described, together with a summary of relevant sections of reverberant chamber theory, as re-applied to a water-filled tank. Techniques for using the tank for determining the acoustical power output and directivity of sound sources are described, from both a theoretical and a practical viewpoint. Particular attention is given to the complicating effects of spatial and spectral variability, and a description is given of the means of accounting for these effects. Methods for improving the tank properties are discussed.

## RELEASE LIMITATION

*Approved for public release*

*HIGH QUALITY PRINTING*

DEPARTMENT OF DEFENCE

DEFENCE SCIENCE AND TECHNOLOGY ORGANISATION

19960806 030

*Published by*

*DSTO Aeronautical and Maritime Research Laboratory  
GPO Box 4331  
Melbourne Victoria 3001*

*Telephone: (03) 626 8111  
Fax: (03) 626 8999*

*© Commonwealth of Australia 1996  
AR No. 009-476  
January 1996*

**APPROVED FOR PUBLIC RELEASE**

## *Executive Summary*

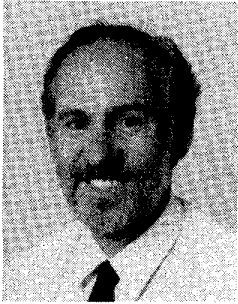
This document describes the acoustical properties of the test tank of the Maritime Operations Division at DSTO Salisbury, and establishes its usefulness for both CW (continuous, single frequency emission) and broadband sonar testing. The document includes, in an easy to read form, descriptive information on techniques to use to obtain measurements, of pre-determined accuracy, in the MOD Salisbury test tank. Particular attention is paid to the measurement of sound source strength and directivity, to the accounting of the complicating effects of spatial and spectral variability, and to the frequency limits of validity.

The methods used to determine the properties of the MOD Salisbury test tank are described in sufficient detail and generality for others to similarly characterise different water-filled acoustical test chambers. This description includes a review of the relevant theory of reverberant chambers. It is believed that there is no other single reference in the literature, in which each of room acoustic theory, spatial variability and spectral variability are described, and in which a practical guide is given to the use of a reverberant chamber, whether water or air-filled, for acoustical measurements.

In view of the expense of alternate reservoir and sea-based hydrophone and projector calibration procedures, the derivation of the limits of applicability of the MOD Salisbury test tank is particularly useful. Also, in reference to the present consideration being given to moving the Salisbury tank, or constructing a new facility, the general description of the acoustics of water-filled chambers, which is included in this document, will provide a vital source of information in the event that a new chamber is designed, or in the event that the location and, hence, properties of the present tank are changed.

## Authors

### **Adrian D. Jones** Maritime Operations Division



*Adrian Jones is a Senior Research Scientist at MOD Salisbury. He joined DSTO in 1987 after working for 9 years in research relating to the acoustics and gas dynamics of engine exhausts. At MOD his work has included the development of software for sonar system studies, research into ocean environmental acoustics and the study of the effects of the environment on the performance of sonar systems. Presently he leads a group engaged in Underwater Operations Research.*

---

### **Stephen A. Hoefs** Maritime Operations Division

*Stephen Hoefs has worked for the Defence Science and Technology Organisation since 1987 as a research engineer focussing on underwater transducers. Stephen has published papers on hydrodynamics of towed arrays and towed underwater projectors. He has participated in several large scale international trials investigating Matched Field Processing and Towed Array Performance. He now heads the scientific group managing the First of Class sonar sea trials for Australia's new submarine, HMAS Collins.*

---

# Contents

1.	INTRODUCTION	1
2.	SUMMARY OF ACOUSTICS OF REVERBERANT CHAMBERS	2
2.1	<i>Introduction</i>	2
2.2	<i>Reverberation time</i>	3
2.3	<i>Sabine Equation</i>	4
2.4	<i>Direct and Reverberant Sound Field Contributions</i>	5
2.5	<i>Sound Power Measurements in Tank</i>	6
2.6	<i>The MOD Salisbury Test Tank as a Reverberant Chamber</i>	8
2.7	<i>Averaging of Spatial Variability</i>	13
2.8	<i>Averaging of Spectral Variability</i>	17
2.9	<i>Lower Frequency Limit</i>	20
2.10	<i>Upper Frequency Limit</i>	21
3.	MEASUREMENTS AND ESTIMATION OF ACOUSTICAL PROPERTIES OF MOD SALISBURY TEST TANK	22
3.1	<i>Water-Wall Pressure Amplitude Reflection Coefficient Measurements</i>	23
3.1.1	<i>using the elliptical geometry of the tank</i>	23
3.1.2	<i>reflection coefficient measurements</i>	25
3.2	<i>Water-Air Pressure Amplitude Reflection Coefficient Estimation</i>	26
3.3	<i>Estimation of Tank Sound Power Absorption Coefficient</i>	28
3.4	<i>Estimated Reverberation Times</i>	29
3.5	<i>Measured Reverberation Times</i>	30
3.6	<i>Reverberation Radius Determined from Measurements</i>	33
3.7	<i>Effect of Changing Absorption of Tank Walls</i>	35
3.7.1	<i>increasing absorption</i>	35
3.7.2	<i>decreasing absorption</i>	36
4.	PROCEDURES FOR MEASUREMENTS	36
4.1	<i>SL and Sound Power Measurements</i>	36
4.1.1	<i>direct sound field</i>	37
4.1.2	<i>reverberant sound field</i>	38
4.2	<i>Directivity Measurements</i>	39
4.2.1	<i>source directivity</i>	39
4.2.2	<i>receiver directivity</i>	40
4.3	<i>Spatial Averaging</i>	40
4.4	<i>Spectral Averaging</i>	41
4.5	<i>Lower Limiting Frequency</i>	42
4.6	<i>Upper Limiting Frequency</i>	42
4.7	<i>Measurements of Reverberation Time</i>	43
5.	CONCLUSIONS	44
	REFERENCES	46

## List of Tables

Table 1: *Measured Spatial Separation for  $e^{-1}$  Autocorrelation of Mean Square Pressure, for MOD Salisbury Test Tank* 11

<b>Table 2:</b>	<i>Test of Hypothesis: Spatial Distribution of RMS Pressure Measured in MOD Salisbury Test Tank fits Rayleigh Distribution (95% confidence)</i>	<b>12</b>
<b>Table 3:</b>	<i>Sound Field Properties at Different Fractions of Reverberation Radius, <math>r_0</math></i>	<b>16</b>
<b>Table 4:</b>	<i>Measurements of Normal Incidence Pressure Amplitude Reflection Coefficient, <math>R_{wall}</math>, MOD Salisbury Test Tank</i>	<b>26</b>
<b>Table 5:</b>	<i>Wall Reflection and Absorption Coefficients, MOD Salisbury Test Tank</i>	<b>28</b>
<b>Table 6:</b>	<i>Estimated Average Sound Absorption Coefficients for MOD Salisbury Test Tank</i>	<b>29</b>
<b>Table 7:</b>	<i>Estimated Reverberation Times for MOD Salisbury Test Tank, <math>T_{60}</math> (ms)</i>	<b>29</b>
<b>Table 8:</b>	<i>Measured &amp; Estimated Reverberation Times, <math>T_{60}</math>, for MOD Salisbury Test Tank (ms)</i>	<b>33</b>
<b>Table 9:</b>	<i>Effective &amp; Estimated Sound Absorption Coefficients for MOD Salisbury Test Tank</i>	<b>34</b>
<b>Table 10:</b>	<i>Reverberation Radius, <math>r_0</math>, Based on Measured Reverberation Time, MOD Salisbury Test Tank (for omnidirectional sound sources)</i>	<b>35</b>

### List of Figures

<b>Figure 1:</b>	<i>Projector Location in Vertical Plane, MOD Salisbury Test Tank</i>	<b>9</b>
<b>Figure 2:</b>	<i>Projector Location in Horizontal Plane, MOD Salisbury Test Tank</i>	<b>9</b>
<b>Figure 3:</b>	<i>Spatial variation of sound pressure measured along straight line in MOD Salisbury test tank with source at fixed location: (a) source frequency 1 kHz, (b) 2 kHz</i>	<b>10</b>
<b>Figure 4:</b>	<i>Spatial variation of sound pressure measured along straight line in MOD Salisbury test tank with source at fixed location: (c) source frequency 4 kHz, (d) 8 kHz</i>	<b>11</b>
<b>Figure 5:</b>	<i>Autocorrelation of mean square of sound pressure measured along straight line in MOD Salisbury test tank with source at fixed location: (a) source frequency 1 kHz, (b) 2 kHz</i>	<b>12</b>
<b>Figure 6:</b>	<i>Autocorrelation of mean square of sound pressure measured along straight line in MOD Salisbury test tank with source at fixed location: (c) source frequency 4 kHz, (d) 8 kHz</i>	<b>13</b>
<b>Figure 7:</b>	<i>Distribution of spatial variation of sound pressure level measured along straight line in MOD Salisbury test tank with source at fixed location (jagged line), compared with theory for Rayleigh distributed rms pressure values (smooth curve): (a) source frequency 1 kHz, (b) 2 kHz</i>	<b>14</b>
<b>Figure 8:</b>	<i>Distribution of spatial variation of sound pressure level measured along straight line in MOD Salisbury test tank with source at fixed location (jagged line), compared with theory for Rayleigh distributed rms pressure values (smooth curve): (c) source frequency 4 kHz, (d) 8 kHz</i>	<b>15</b>
<b>Figure 9:</b>	<i>Spectral variation of sound pressure measured in MOD Salisbury test tank with source and receiver at fixed locations: swept sine source frequency 1400 - 2600 Hz</i>	<b>18</b>
<b>Figure 10:</b>	<i>Autocorrelation of linear rms sound pressure measured in MOD Salisbury test tank with source and receiver at fixed locations: sine sweep source frequency 1400 - 2600 Hz; for 0 - 50 Hz frequency displacement</i>	<b>18</b>

- Figure 11: Distribution of spectral variation of sound pressure level measured in MOD Salisbury test tank with source and receiver at fixed locations (jagged line), compared with theory for Rayleigh distributed rms pressure values (smooth curve): sine sweep source frequency 1400 - 2600 Hz* **19**
- Figure 12: Experimental Setup in Plan View & Typical Output Signal, MOD Salisbury Test Tank* **24**
- Figure 13: Sound Intensity Area Ratios* **25**
- Figure 14: Hydrophone Output At 4 kHz, MOD Salisbury Test Tank* **26**
- Figure 15: Water - Air Interface* **27**
- Figure 16: Reverberant decay of instantaneous pressure at fixed receiver in MOD Salisbury Test Tank @ 1 kHz* **30**
- Figure 17: MOD Salisbury test tank reverberant decay curves integrated in time: (a) at source frequency 1 kHz, (b) 2 kHz. The measured decay curves are depicted by dashed lines. The dotted lines are an estimate of a uniform decay rate for use in the analysis.* **31**
- Figure 18: MOD Salisbury test tank reverberant decay curves integrated in time: (c) at source frequency 4 kHz, (d) 8 kHz. The measured decay curves are depicted by dashed lines. The dotted lines are an estimate of a uniform decay rate for use in the analysis.* **32**

## List of Symbols

$a$	intensity absorption coefficient, dB/m
$A$	pressure amplitude of right-travelling sound wave, Pa, total surface area of tank boundaries, m <sup>2</sup>
$Area$	area of box depicting the sound intensity at various distances from the projector, m <sup>2</sup>
$B$	pressure amplitude of left-travelling sound wave, Pa
$c$	sound velocity, m/s
$e$	base of natural logarithms (2.71828...)
$f$	frequency, Hz
$f_{max}$	upper frequency limit, Hz
$f_{Sch}$	Schroeder cutoff frequency, Hz
$(\Delta f)_{mode}$	average spacing between successive chamber resonance frequencies, Hz
$(\Delta f)_{res}$	bandwidth of chamber resonance, Hz
$j$	imaginary unit, $\sqrt{-1}$
$k$	wave number $\omega/c$ , rad/m
$L$	separation distance between receivers in tank, m
$N$	number of modes for reverberant chamber
$N_{samp}$	number of independent samples of sound pressure level obtained in tank
$p$	instantaneous acoustical pressure, Pa
$p_{ref}$	reference acoustic pressure, 1 $\mu$ Pa (20 $\mu$ Pa for air acoustics)
$\overline{p_{dir}}^2$	mean square acoustical pressure in direct field, Pa <sup>2</sup>
$\overline{p_{rev}}^2$	spatially averaged mean square acoustical pressure in reverberant field, Pa <sup>2</sup>
$P$	time-averaged sound power radiated by acoustic source, W
$P_d$	time-averaged sound power dissipated at boundary surfaces of chamber, W
$P_{direct}$	pressure amplitude of the direct signal from the projector, Pa
$P_{reflect}$	pressure amplitude of the reflected signal, Pa
$Q_\theta$	directivity of sound source, non-dimensional
$r$	distance from sound source, m
$r_0$	radius of reverberation - distance from projector at which average energy densities of direct and reverberant fields are equal, m
$R_{air}$	normal incidence pressure amplitude reflection coefficient at the water to air interface
$R_{rc}$	room constant, m <sup>2</sup>
$R_{wall}$	normal incidence pressure amplitude reflection coefficient at the water to tank wall interface
$S$	total surface area of the tank boundaries, m <sup>2</sup>
$SPL_{dir}$	rms sound pressure level due to direct field, dB re 1 $\mu$ Pa
$SPL_{rev}$	sound pressure level of spatially averaged rms sound pressure due to reverberant field, dB re 1 $\mu$ Pa
$t$	time, seconds
$T_{ref}$	arbitrarily chosen constant
$T_{60}$	reverberation time (time for acoustic energy density to decay 60 dB), seconds

$u$	instantaneous acoustical particle velocity, m/s
$V$	volume of water in tank, m <sup>3</sup>
$\bar{w}$	time-averaged acoustic energy density in chamber, W/m <sup>3</sup>
$\bar{w}_{dir}$	time-averaged acoustic energy density due to direct field, W/m <sup>3</sup>
$\bar{w}_{rev}$	time-averaged acoustic energy density due to reverberant field, W/m <sup>3</sup>
$W$	averaging bandwidth, Hz
$x$	distance in direction of propagation of sound wave, m
	constant of proportionality
	is maximum permissible absorption within the fluid, dB
$X$	length of straight line traverse used for receiver, m
ms	millisecond
$\bar{\alpha}$	weighted average sound power absorption coefficient for the entire tank
$\alpha$	pressure amplitude absorption coefficient, nepers/m (at $\frac{1}{\alpha}$ m distance, the pressure amplitude has dropped to $\frac{1}{e}$ of its initial value)
$\alpha_{air}$	sound power absorption coefficient at the water to air interface
$\alpha_e$	effective absorption coefficient derived from the sabine equation using measured reverberation times
$\alpha_{wall}$	sound power absorption coefficient at the tank wall
$\beta_{wall}$	sound power reflection coefficient at the water to tank wall interface (based on the square of the pressure amplitude ratio)
$\beta_{air}$	sound power reflection coefficient at the water to air interface (based on the square of the pressure amplitude ratio)
$\eta$	coefficient of shear viscosity, Pa · s
$\eta_B$	coefficient of bulk viscosity, Pa · s
$\lambda$	wavelength, m
$\rho$	fluid density, kg/m <sup>3</sup>
$\sigma$	standard deviation for probability distribution, dB
$\sigma_{res}$	standard deviation for probability distribution resulting from spatial or spectral averaging, dB
$\tau$	time for acoustic energy density to decay by factor $e^{-1}$ , s
$\omega$	angular frequency, rad/s

#### Subscripts

1	water
2	air
<i>dir</i>	direct field component
<i>i</i>	incident sound wave,
	<i>i</i> th part of tank boundary surface
<i>r</i>	reflected sound wave
<i>rev</i>	reverberant field component
<i>t</i>	transmitted sound wave

# *Acoustical Properties of the MOD Salisbury Test Tank and Techniques for Measurements*

## *1. Introduction*

This document describes work which has established the limits of usefulness of the test tank of the Maritime Operations Division at DSTO Salisbury for both CW (continuous, single frequency emission) and broadband sonar testing. The document also reports, in an easy to read form, descriptive information on techniques to use for measurements in the MOD Salisbury test tank. The work described in this document is, in fact, a serendipitous spin-off from a detailed investigation of the effects of spatial and spectral variability on the performance of sonar systems. The present work was completed to the degree reported below, as it was realised that the MOD Salisbury test tank had never before been characterised acoustically, and as the limitations on its use were previously unknown.

The MOD Salisbury test tank was found to behave as a reverberant chamber. The relevant theory of reverberant chambers is then reviewed below, as the authors believe that there is no single reference in the literature, in which each of room acoustic theory, spatial variability and spectral variability are described, and in which a practical guide is given to the use of a reverberant chamber for acoustical measurements. Also, the review of this material is necessary as it places the work performed in context, and as it clarifies the basic assumptions from which the measurement procedures are derived. For the convenience of MOD personnel, all theoretical aspects are presented in terms of a water-filled chamber, as many equations presented elsewhere in the literature are only relevant for air-filled chambers. No other in-depth description of the properties of water-filled chambers is believed to exist in the literature. This material has relevance to other water-filled acoustic test chambers which exist in the Australian defence community, as the relations presented below are general in nature, and may be applied directly to such chambers, in most cases.

The scientific use of a reverberant acoustic chamber for sound power measurements of noise sources is common in the field of air acoustics and is extensively documented, for example, chapter 9 in reference (1) and chapter 6 in reference (2). The corresponding use of a reverberant water-filled tank in underwater acoustics appears to be uncommon, with most such facilities being used for transient measurements. In fact, it appeared to the authors that the

underwater acoustics community was largely unaware of room acoustics theory. Reference (3), however, briefly describes an example of the use of a water filled tank as a reverberant chamber. It occurred to the authors that the MOD test tank at DSTO Salisbury would act as a reverberant chamber, as both the concrete-lined walls and the air-water interface were expected, by virtue of a high acoustic impedance mis-match, to be acoustically reflective. Further, in view of the expense of alternate reservoir and sea-based hydrophone and projector calibration procedures, it was decided to establish the limits of applicability of the MOD Salisbury test tank, based on the well established principles of air-filled room acoustics.

This acoustical characterisation of the MOD Salisbury test tank, has led to two different test procedures. Firstly, by establishing the distance from a sound source in the tank at which the average sound intensity due to the direct radiated sound is greater than the average sound intensity due to the reverberant sound field (sound reflected from the tank walls and from the air-water interface), a means of obtaining direct field measurements was established. Secondly, by locating a receiver in the reverberant sound field, sufficiently far from the sound source, a means of indirectly measuring the sound power of a source, based on the average rate of sound absorption in the tank, was specified. Vanselow, in reference (3), gives an incomplete description of this second method.

This document describes the MOD Salisbury test tank properties, so as to assist the conduct of measurements in the tank. Further, measured data is used to show how the MOD Salisbury test tank might be modified to improve its utility. A more detailed analysis of the statistical properties of the reverberant sound field in the tank will be included in a future report, as that work relates more directly to the general performance of acoustical receivers and arrays, and to the acoustics of shallow water environments.

## ***2. Summary of Acoustics of Reverberant Chambers***

### ***2.1 Introduction***

The summary of the theory relating to reverberant chambers, which is presented below, is generalised for a fluid-filled chamber, with particular reference to water as the fluid medium. The approach is based mainly on reference (2).

For a fluid-filled chamber, enclosing a single sound source, the sound pressure at a receiver will be a summation of that due to sound travelling directly from the sound source, plus that which emanates from the sound source and travels along paths which involve reflections with the chamber boundaries. Depending upon the sound absorptive properties of the chamber boundaries, the number of paths which involve reflections which contribute significantly to the total sound pressure at the receiver may be either as low as zero or very large. For a true anechoic chamber, all sound incident on the chamber boundaries is absorbed, whereas for a highly reverberant chamber, a large number of reflections contribute to the received pressure, with phase coherent

addition of the components from the direct path and from all the reflected paths being relevant. A highly reverberant chamber thus has multi-path acoustic transmission from a sound source to a receiver, and may be regarded as a multi-modal environment. Clearly, the closer a receiver is to the sound source, the greater is the contribution from the direct sound path.

This will be true for any acoustical wavelength, however, for wavelengths which are much larger than chamber dimensions, significant reflections from the chamber boundaries reach the sound source at more or less the same phase (the air-water interface will cause a  $180^\circ$  phase change) and act on the source to change the effective radiation impedance. For this reason, as well as other reasons mentioned below, there is a lower frequency limit for the applicability of reverberant chamber theory. Generally speaking, chamber dimensions need to be greater than a wavelength. In the case of the MOD Salisbury test tank, for a maximum chamber dimension (length) of 7.5 m, this restriction implies a lower frequency limit of approximately 200 Hz.

## 2.2 Reverberation time

For a chamber with reflective boundaries, if there is no sound absorption within the fluid<sup>1</sup> and all absorption occurs upon incidence with the boundaries, the relation between the rate of change of the energy density (in the reverberant field) in the chamber,  $\frac{d\bar{w}}{dt}$ , the acoustic power supplied by a sound source,  $\bar{P}$ , and the power dissipated at the boundary surfaces,  $\bar{P}_d$ , from the requirement for the conservation of acoustical energy, is given by (from reference (2))

$$V \frac{d\bar{w}}{dt} = \bar{P} - \bar{P}_d . \quad (1)$$

where  $V$  is volume of water in tank,  $\text{m}^3$

For each relevant term in equation (1), the bar indicates a running time average.

The relation between the sound power dissipated and the acoustic energy density in the reverberant field is given by (reference (2)):

$$\bar{P}_d = \frac{c}{4} \bar{\alpha} A \bar{w} \quad (2)$$

where  $c$  is sound velocity,  $\text{m/s}$

$\bar{\alpha}$  is weighted average sound power absorption coefficient for the entire tank

$A$  is total surface area of tank boundaries,  $\text{m}^2$

The factor, 4, in equation (2) results from the assumption that the reverberant sound field is perfectly diffuse, that is, an equal amount of sound energy is

<sup>1</sup> In the theoretical approach presented below, it is assumed that no absorption of sound takes place within the fluid. The absorption of sound in the fluid medium imposes an upper frequency limit on the use of a reverberant chamber, and is discussed in section 2.10.

presumed to be travelling in every direction within the sound field. The derivation of this factor is similar to the explanation given in section 9.2.2 of reference (1).

By substitution, the equation for energy conservation, equation (1), then becomes

$$V \frac{d\bar{w}}{dt} + \frac{c}{4} \bar{\alpha} A \bar{w} = P . \quad (3)$$

From equation (3) it may be shown that, following the sudden removal (cessation) of the sound source, in the case of a fully insonified chamber, the acoustic energy density in the chamber will undergo an exponential decay, as the remaining acoustical energy is progressively absorbed. The characteristic decay time,  $\tau$ , being the time for the acoustical energy density to decrease by a factor  $e^{-1}$ , is then given by

$$\tau = \frac{4V}{c\bar{\alpha}A} . \quad (4)$$

In the case of room acoustics, it is common to use the term,  $T_{60}$ , or reverberation time, this being the time for the acoustic energy density to decrease by 60 dB (i.e decrease by a factor of  $10^6$ ). It follows that  $T_{60} = (6 \ln 10)\tau = 13.82\tau$ , that is, we have

$$T_{60} = \frac{24V \ln 10}{c\bar{\alpha}A} . \quad (5)$$

In the case of a speed of sound for fresh water of 1481 m/s (appendix 10, reference (4)), the reverberation time becomes

$$T_{60} = \frac{0.0373 V}{\bar{\alpha}A} . \quad (6)$$

### 2.3 Sabine Equation

For practical acoustical chambers, it is assumed that each of the  $i$  parts of the chamber boundary surface, of surface area  $A_i$ , has associated with it a particular sound absorption coefficient  $\alpha_i$ . The overall sound absorption coefficient for the chamber,  $\bar{\alpha}$ , is assumed to be given by

$$\bar{\alpha} = \frac{\sum_i \alpha_i A_i}{A} . \quad (7)$$

The Sabine equation (named in honour of W. C. Sabine - reference (2)) for the reverberation time of a water-filled chamber then follows from equation (6) as

$$T_{60} = \frac{0.0373 V}{\sum_i \alpha_i A_i} . \quad (8)$$

As shown in section 3, for a particular chamber the reverberation time may be estimated, based on the known, calculated or measured acoustical absorption coefficients for the different boundary surfaces of the chamber. Further, as shown below, a determination of the reverberation time, by either measurement or estimation, coupled with a knowledge of the chamber volume

and the surface area of its boundaries, leads to the complete acoustical characterisation of the chamber.

## 2.4 Direct and Reverberant Sound Field Contributions

For a sound source in a reverberant acoustical chamber, the sound pressure received at a particular point in the chamber is due to a contribution from the directly radiated sound and due to contributions from the sound received along all the paths which involve sound reflections at a boundary surface. There will be an infinite number of these latter contributions, but their significance will, of course, be related to the degree of sound absorption occurring at each reflection. For the direct field component, for a sound source of directivity  $Q_\theta$ , the acoustical energy density  $\overline{w}_{dir}$  at a distance  $r$  from the acoustic centre of the source is given by free field sound radiation considerations as

$$\overline{w}_{dir} = \frac{P Q_\theta}{4\pi r^2 c}. \quad (9)$$

For the reverberant sound field, we may make use of equation (2). This obtains the relation between the power dissipated within the room and the acoustic energy density. Now, the rate at which acoustic power is being added to the reverberant field is  $(1 - \bar{\alpha})P$ , as the addition to the reverberant field occurs after the first reflection from the chamber boundary surfaces. Since, for a steady state situation, with no change to the rate of energy addition by the source, the rate at which energy is being added to the chamber is equal to the rate at which it is dissipated, we have the result that the energy density  $\overline{w}_{rev}$  due to the reverberant field (at any location in the room) is given by

$$\overline{w}_{rev} = \frac{4 P}{c R_{rc}}, \quad (10)$$

$$\text{where } R_{rc} = \frac{\bar{\alpha} A}{1 - \bar{\alpha}} \quad (11)$$

is known as the room constant.

For later convenience  $R_{rc}$  may be expressed in terms of the reverberation time  $T_{60}$ . Here, substitutions may be made in equation (11) using equations (7) and (8), giving

$$R_{rc} = \frac{0.0373 V}{T_{60} - 0.0373 V/A} \quad (12)$$

As mean square pressure is equal to  $pc^2$  times the acoustical energy density (this follows, for example, from equation (5.62) of reference (4)), the total mean square acoustical pressure  $\overline{p^2}$  at a distance  $r$  from the sound source, resulting from both the direct and reverberant contributions, from equations (9) and (10), follows<sup>2</sup> as

---

<sup>2</sup> Note that a value of mean square acoustical pressure is wholly real, and thus subject to phase cancellations, and hence requires spatial averaging.

$$\overline{p^2} = \rho c P \left( \frac{Q_0}{4\pi r^2} + \frac{4}{R_c} \right). \quad (13)$$

where  $\rho$  is fluid density,  $\text{kg/m}^3$

Now, at a particular distance from the sound source, the contributions from the direct and reverberant sound fields will be equal. From equation (13), it follows that this distance, known as the radius of reverberation, or critical radius,  $r_0$ , is given by

$$r_0 = \sqrt{\frac{R_c Q_0}{16\pi}}. \quad (14)$$

Using equation (12), the reverberation radius in a water-filled chamber may then be expressed conveniently in terms of the reverberation time, as

$$r_0 = \sqrt{\frac{0.0373 V Q_0}{16\pi (T_{60} - 0.0373 V/A)}}. \quad (15)$$

## 2.5 Sound Power Measurements in Tank

In terms of acoustical measurements obtained in the water-filled test tank, if a receiver is located at a distance from a sound source which is much less than  $r_0$ , then the acoustical pressure measured will correspond with that obtained at the same distance in a free field environment. This situation corresponds with the reverberant sound component disappearing from equation (13). The sound power  $P$  of the source then follows as

$$P = \frac{4\pi r^2 \overline{p_{dir}^2}}{\rho c Q_0}. \quad (16)$$

where  $\overline{p_{dir}^2}$  is mean square acoustical pressure in direct field,  $\text{Pa}^2$

Conversely, if the receiver is located much further from the source than  $r_0$ , the acoustical pressure measurements will correspond with the reverberant sound field in the tank. Here the sound power of the source may also be determined. In this case, the direct field component disappears from equation (13) and the sound power  $P$  is obtained as

$$P = \frac{R_c \overline{p_{rev}^2}}{4\rho c}. \quad (17)$$

where  $\overline{p_{rev}^2}$  is spatially averaged mean square acoustical pressure in reverberant field,  $\text{Pa}^2$

Using equations (16) and (17), it is possible to relate measurements of mean square sound pressure in either of the direct or the reverberant fields to the absolute power output of an acoustical source, expressed as watts. Alternatively, with re-arrangement, the power output may be expressed as the source level,  $SL$ . (From, for example, section 8.9 of reference (4), the  $SL$  of an

acoustical source is defined as the axial response, as an rms sound pressure level in dB, extrapolated back to a position 1 m from the acoustical centre of the source.)

From equation (16), setting  $Q_0$  to 1 (to give the axial response), using values of density and sound velocity for fresh water of  $998 \text{ kg/m}^3$  and  $1481 \text{ m/s}$ , respectively (appendix 10 of reference (4)), and using a reference sound pressure level of  $1 \mu\text{Pa}$ , the direct field rms sound pressure level,  $SPL_{dir}$ , may be given as a function of source sound power  $P$  and measurement distance  $r$  as

$$SPL_{dir} = 170.7 + 10 \log_{10} P - 20 \log_{10} r \text{ dB} \quad (18)$$

where  $SPL_{dir}$  is rms sound pressure level due to direct field, dB re  $1 \mu\text{Pa}$ , that is

$$SPL_{dir} = 10 \log_{10} \left( \frac{\overline{p_{dir}}^2}{\overline{p_{ref}}^2} \right)$$

where  $p_{ref}$  is reference acoustic pressure,  $1 \mu\text{Pa}$  ( $20 \mu\text{Pa}$  for air acoustics)

If a direct field measurement at 1 m distance is possible, the  $SL$  is then the same as the measured rms sound pressure level. For other measurement distances, the  $SL$  may be obtained with the distance correction implied by equation (18). It is worth noting that the  $SL$  may thus be determined from a measurement of the direct field sound pressure level,  $SPL_{dir}$ , taken at any distance from a monopole source existing as a pulsating sphere. Such a measurement may even be taken at a point on the surface of the sphere, regardless of the acoustic wavelength (so long as the displacement of the surface is much less than the radius of the sphere). (See, for example, section 8.1 of reference (4).) The commonly held view that a measurement must be taken at least one wavelength from the source is then false.

From equation (18), the  $SL$  follows as

$$SL = 170.7 + 10 \log_{10} P \text{ dB}$$

Substituting for  $P$ , using equation (17), and re-introducing  $Q_0$  from equation (16) via equation (18) (which we must do as our measurement of  $SPL_{rev}$  is not referenced to on-axis response) gives an expression for  $SL$ , based on a measurement of the rms sound pressure level in a reverberant field,  $SPL_{rev}$ , as

$$SL = SPL_{rev} + 10 \log_{10} R_{rc} + 10 \log_{10} Q_0 - 17.0 \text{ dB}. \quad (19)$$

where  $SPL_{rev}$  is sound pressure level of spatially averaged rms sound pressure due to reverberant field, dB re  $1 \mu\text{Pa}$ , that is

$$SPL_{rev} = 10 \log_{10} \left( \frac{\overline{p_{rev}}^2}{\overline{p_{ref}}^2} \right)$$

By now substituting for the room constant  $R_{rc}$  in terms of the reverberation time  $T_{60}$ , using equation (12), we have an expression for  $SL$  in terms of the volume of water in the tank,  $V$ , and the surface area of the tank boundaries,  $A$ ,

as

$$SL = SPL_{rev} + 10 \log_{10} V + 10 \log_{10} Q_\theta - 10 \log_{10} \left( T_{60} - \frac{0.0373V}{A} \right) - 31.3 \text{ dB.} \quad (20)$$

As discussed below, a value of  $SPL_{rev}$  must be obtained from a measurement procedure which includes either spatial or spectral averaging, or both.

Note that, if  $SL$  has been determined from a direct field measurement using equation (18), a measurement of the rms sound pressure level in the reverberant field,  $SPL_{rev}$ , may be used with equation (20) to determine the directivity,  $Q_\theta$ , of a sound source. Equations (18) and (20) are thus very important in the characterisation of sound sources.

## 2.6 The MOD Salisbury Test Tank as a Reverberant Chamber

The analysis contained in sections 2.2 to 2.5 is applicable to the MOD Salisbury test tank, so long as the tank acts as a reverberant chamber in which the sound field is diffuse. The sound field within the tank was, in fact, confirmed as being diffuse by comparing the observed spatial variability to that which is expected for reverberant chambers. These measurements, in turn, reveal the extent of the measurement problem due to variability of pressure with spatial location, and are shown below to illustrate the problem, and to confirm the accuracy of the diffuse field assumption for the MOD Salisbury test tank.

As is well known and shown, for example, by Pierce (equation 6-7.14 of reference (2)), above the Schroeder cutoff frequency (see section 2.9, below), the mean square pressure response to a pure-tone excitation in a fluid-filled chamber follows an exponential distribution. As shown by Dyer (reference (5)), for example, pressure values for which the mean squares are exponentially distributed follow a Rayleigh density when transformed to rms values. When expressed logarithmically, as dB, these pressure values are distributed with a standard deviation  $\sigma = (10 \log_{10} e) \pi / \sqrt{6} \approx 5.57 \text{ dB}$  (reference (2)). Further, the expected rate of variation with location in the chamber is known. From, for example, Figure 6-18 of Pierce (reference (2)), the spatial autocorrelation function of mean square pressure is given as  $(\sin^2(k \Delta L)) / (k \Delta L)^2$ , where  $k$  is the wave number  $\omega/c$  and  $\Delta L$  is the separation distance of locations in the chamber. Thus, mean square pressure values obtained at  $\lambda/2$  (half wavelength) spacing are statistically independent, and the value of autocorrelation may be shown to fall to  $e^{-1}$  at  $kL = 1.644$ .

The MOD Salisbury test tank has dimensions shown in Figures 1 and 2 below. As shown in Figure 1, viewed in the vertical plane, the tank has vertical sides which are curved (with radius 1 m) at the bottom. Viewed in the horizontal plane at the water-air interface, as shown in Figure 2, the tank has an elliptical shape with major and minor axis dimensions of 7.5 m and 6 m, respectively. The tank is thus shaped like a cylinder of elliptical cross-section, with rounded bottom edges. The volume of the water in the tank is approximately 200 m<sup>3</sup>. The area of the water-air interface (the area of the ellipse) is 35.3 m<sup>2</sup>, with the area of the wetted tank wall being approximately 160 m<sup>2</sup> (the tank bottom area, plus the product of the perimeter of the ellipse and the tank depth).

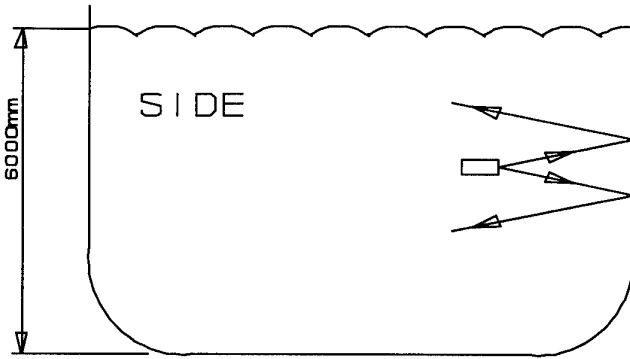


**Figure 1:** Projector Location in Vertical Plane, MOD  
Salisbury Test Tank

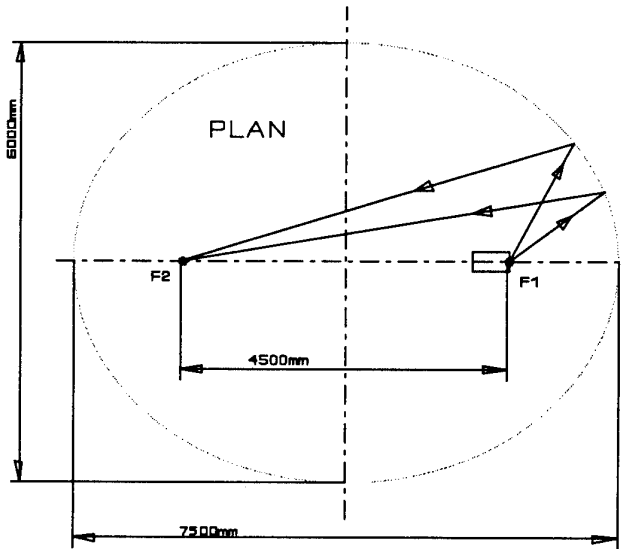


**Figure 2:** Projector Location in Horizontal Plane, MOD  
Salisbury Test Tank

The spatial variability in the MOD Salisbury test tank was measured at each of four frequencies using a fixed source and a moveable hydrophone receiver. In each test, the source emitted a pure tone at one of 1, 2, 4 and 8 kHz. The hydrophone was moved along a vertical line in discrete steps of 0.01 m (0.0053 m for the 8 kHz test) where it was held for a minimum of 15 seconds for each step. The mean square pressure levels were recorded on an HP spectrum analyser using a spectral line separation of 3.125 Hz (flat top windowing) and are shown in Figure 3 for source frequencies 1 and 2 kHz, and in Figure 4 for 4 and 8 kHz. The 15 second pause before each measurement was included to ensure that noise transmitted to the hydrophone by the traversing equipment had decayed. The source and receiver were separated by about 3 m; the vertical traverse started near the bottom of the

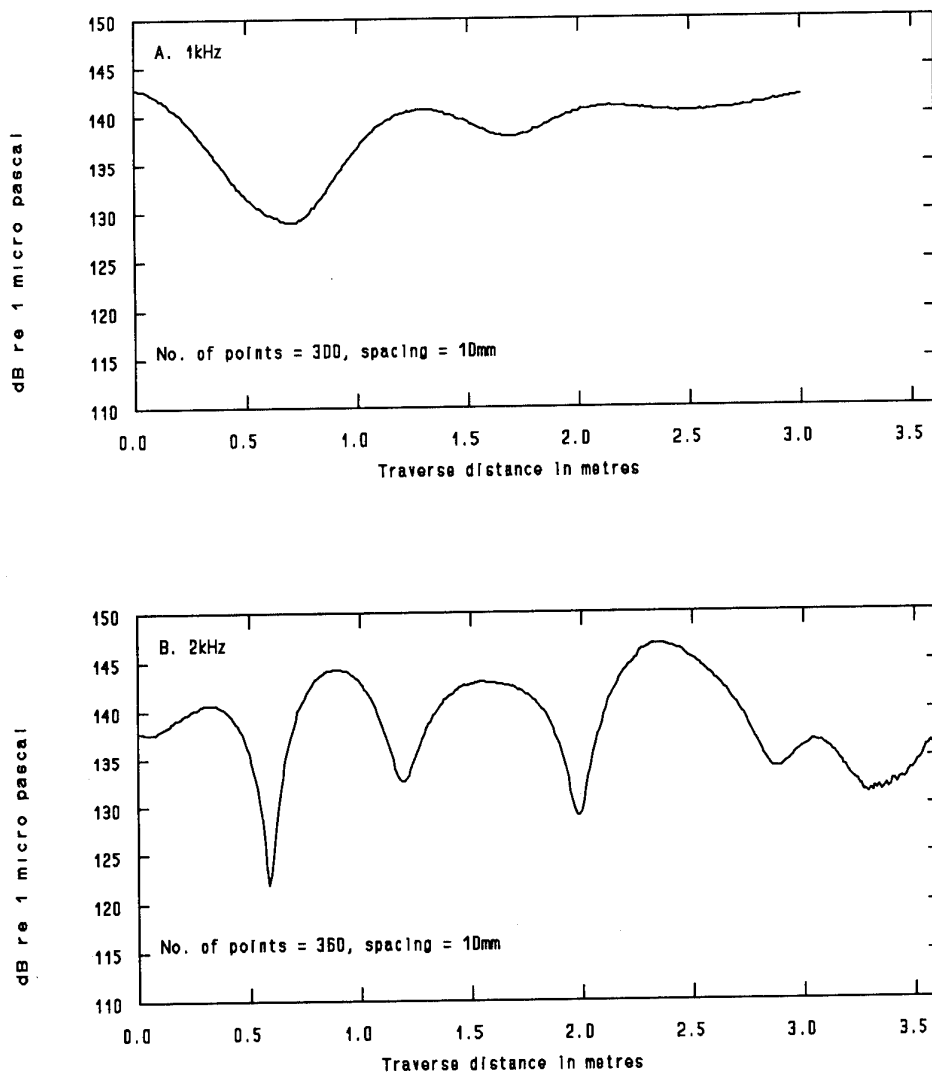


**Figure 3:** Spatial variation of sound pressure measured along straight line in MOD Salisbury test tank with source at fixed location: (a) source frequency 1 kHz, (b) 2 kHz

tank and terminated 1 m from the surface.

Each of the curves of received sound pressure level versus distance shown in Figures 3 and 4 show a large variation with location. The span of values of about 20 dB, for all but the 1 kHz plot in Figure 3, is consistent with the  $\pm 2\sigma$  of 22.3 dB expected for Rayleigh distributed rms pressure values.

Figures 5 and 6 show the corresponding non-dimensional estimates of the autocorrelation function using linear, mean square pressure data. The point at which the autocorrelation reaches  $e^{-1}$  is identified in each of the curves. These values of  $kL$  indicated in Figures 5 and 6 agree very well with the expected value of 1.644 which satisfies the known autocorrelation function for a perfectly diffuse sound field. These values are summarised in Table 1.

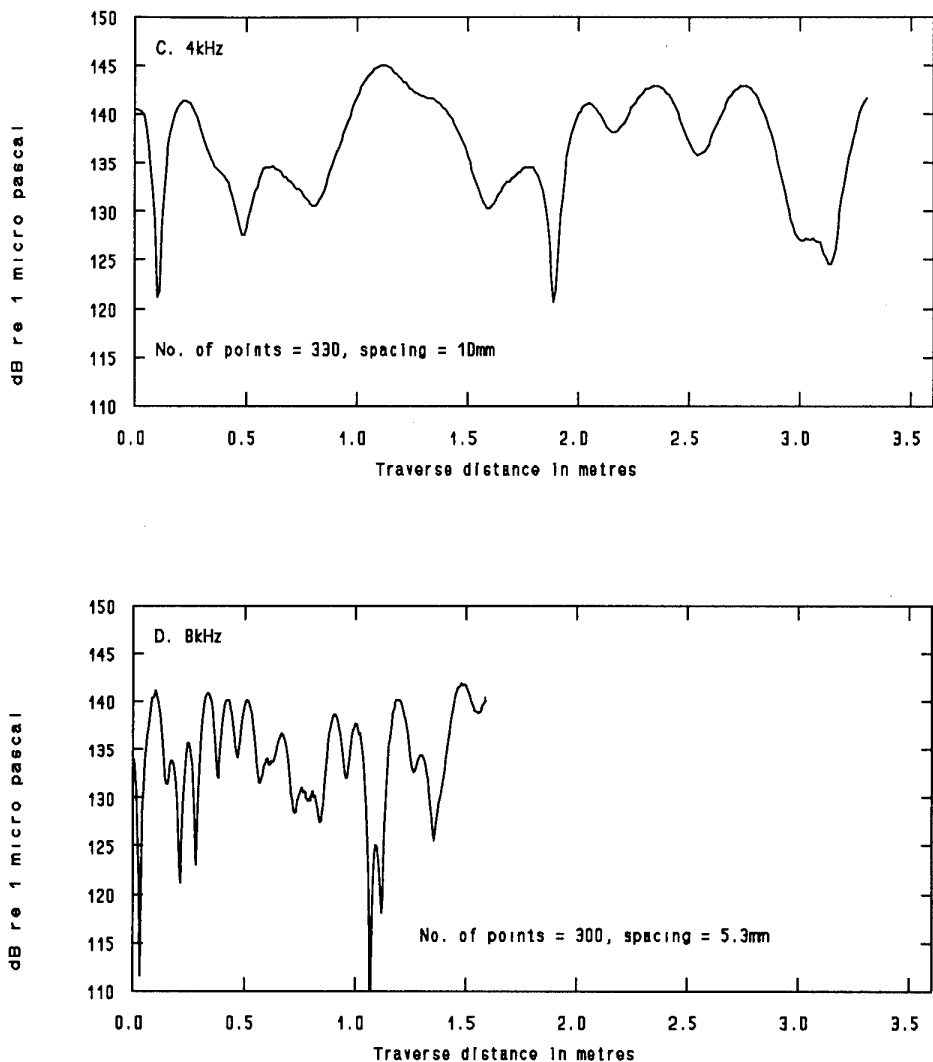
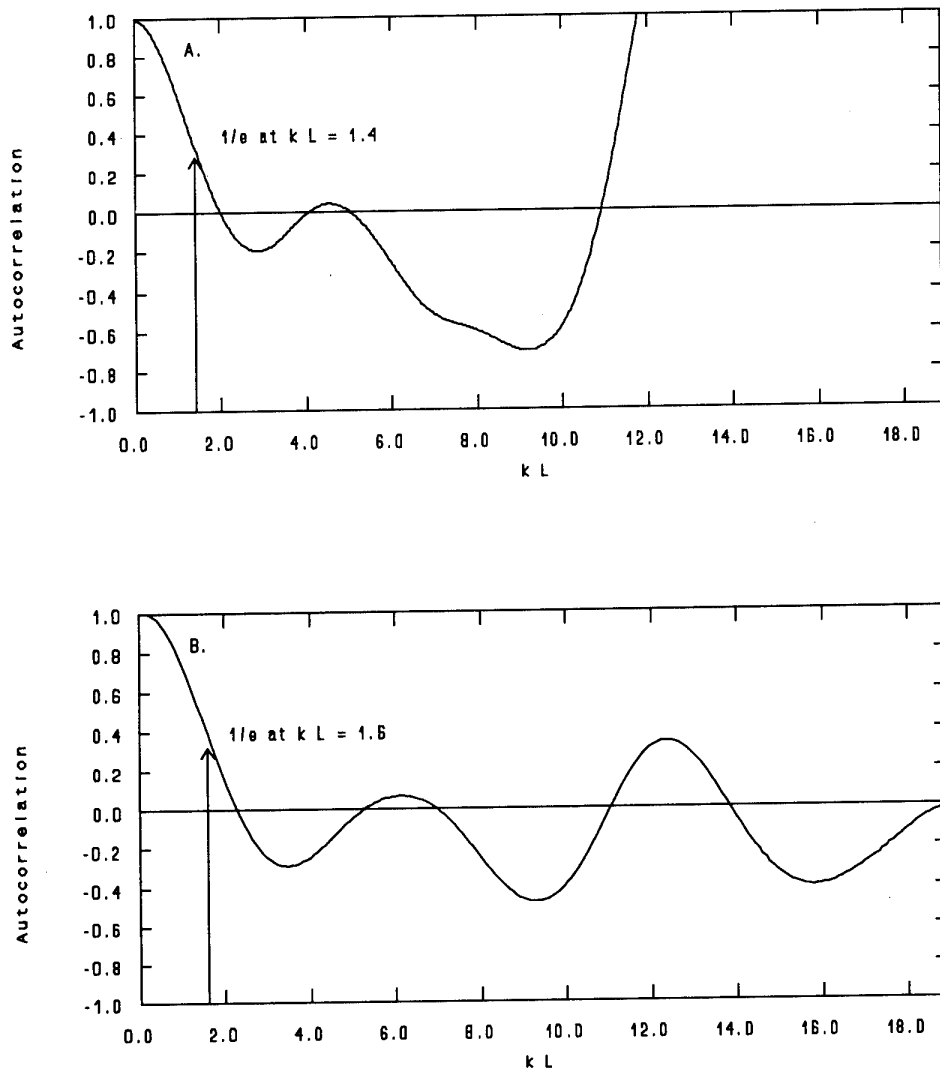


**Figure 4:** Spatial variation of sound pressure measured along straight line in MOD Salisbury test tank with source at fixed location: (c) source frequency 4 kHz, (d) 8 kHz

**Table 1:** Measured Spatial Separation for  $e^{-1}$  Autocorrelation of Mean Square Pressure , for MOD Salisbury Test Tank

Frequency	1000 Hz	2000 Hz	4000 Hz	8000 Hz
$kL$ from theory	1.644	1.644	1.644	1.644
$kL$ measured	1.4	1.6	2.5	1.4

Figures 7 and 8 show the associated probability density functions for sound pressure level generated using uniform class intervals over the range -30 to 10 dB about the mean, as compared with the theoretical probability density associated with Rayleigh distributed rms values given by Dyer (reference (5)).



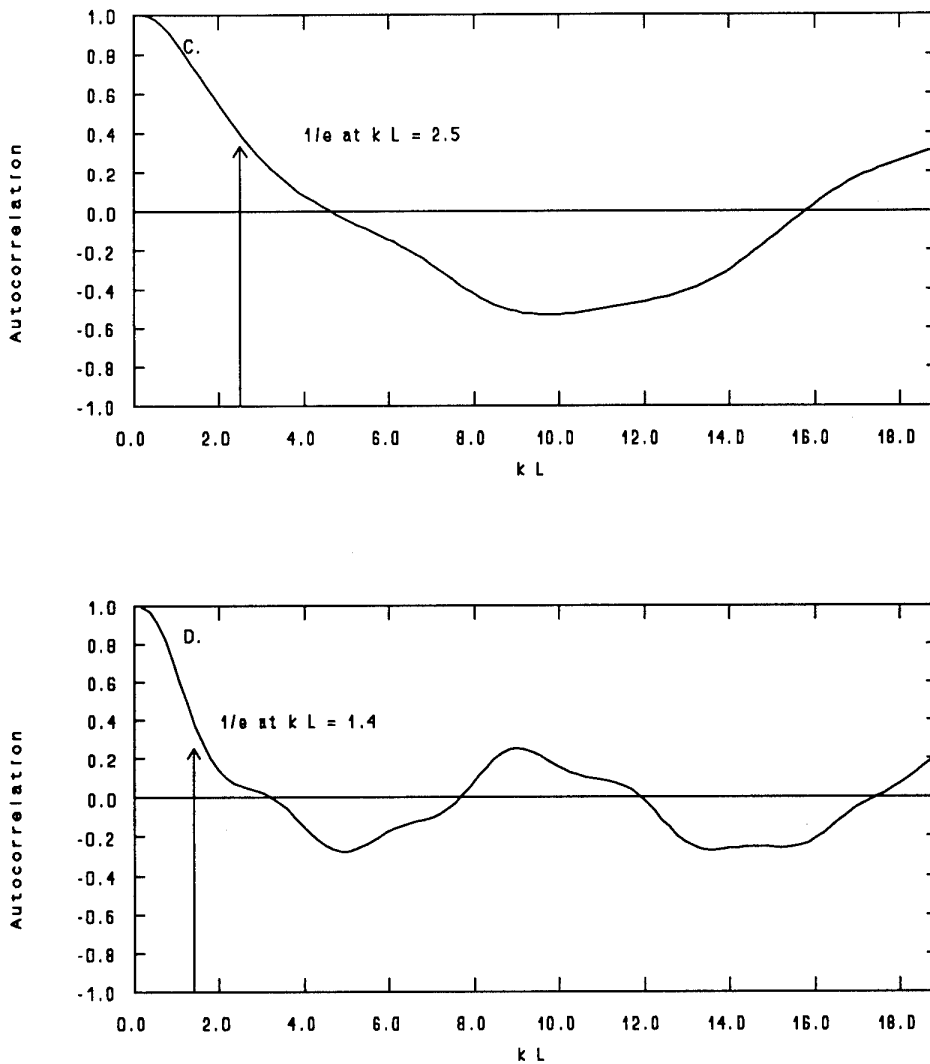
**Figure 5:** Autocorrelation of mean square of sound pressure measured along straight line in MOD Salisbury test tank with source at fixed location: (a) source frequency 1 kHz, (b) 2 kHz

Table 2 lists the results of a  $\chi^2$  goodness-of-fit test for adherence of the measured rms pressure values to the Rayleigh distribution.

**Table 2:** Test of Hypothesis: Spatial Distribution of RMS Pressure Measured in MOD Salisbury Test Tank fits Rayleigh Distribution (95% confidence)

Frequency	1000 Hz	2000 Hz	4000 Hz	8000 Hz
accept or reject	strongly reject	borderline	accept	accept

The conclusion from the results presented in Figures 3 to 8 and Tables 1 and 2 is that the MOD Salisbury test tank is highly diffuse at 1000 Hz and higher frequencies, and that the spatial variations of rms pressure are a good fit to the



**Figure 6:** Autocorrelation of mean square of sound pressure measured along straight line in MOD Salisbury test tank with source at fixed location: (c) source frequency 4 kHz, (d) 8 kHz

Rayleigh distribution for frequencies of 2000 Hz and above. Clearly, the MOD Salisbury test tank may be used as a highly reverberant chamber.

## 2.7 Averaging of Spatial Variability

In practical use, the distance of a receiver from the sound source will be neither much greater nor much less than the radius of reverberation,  $r_0$ , and both the direct and reverberant sound fields will contribute to the received acoustic pressure. For a sound source radiating at a single frequency at a fixed location in a highly reverberant chamber, the reverberant sound field will have a spatially correlated variability of rms pressure corresponding with a Rayleigh probability distribution, as shown above. In the case of both the direct and

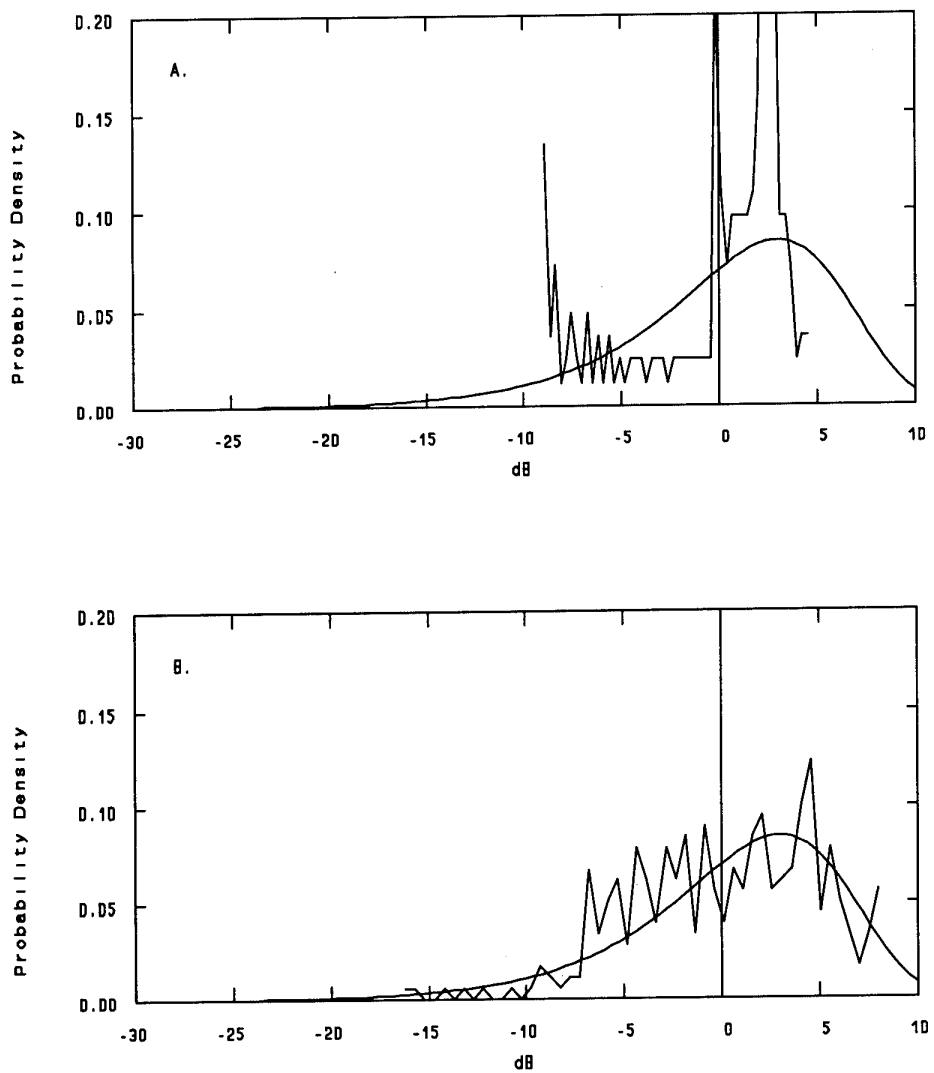


**Figure 7:** Distribution of spatial variation of sound pressure level measured along straight line in MOD Salisbury test tank with source at fixed location (jagged line), compared with theory for Rayleigh distributed rms pressure values (smooth curve): (a) source frequency 1 kHz, (b) 2 kHz

reverberant sound fields contributing to the received sound pressure, the situation is then of a constant vector plus a large number of random vectors, with the spatial variability of the rms pressure now corresponding to a Rician probability distribution (chapter 4, reference (6), for example). In such a spatially variable sound field, the received sound pressure may be averaged over a straight line path which is longer than the distance for the autocorrelation function for mean squared pressure to fall to zero. This distance is half a wavelength for an omnidirectional receiver in a perfectly diffuse sound field (section 6-8 of reference (2), for example).

If spatial averaging is used, it must be remembered that at distance  $r_0$  the

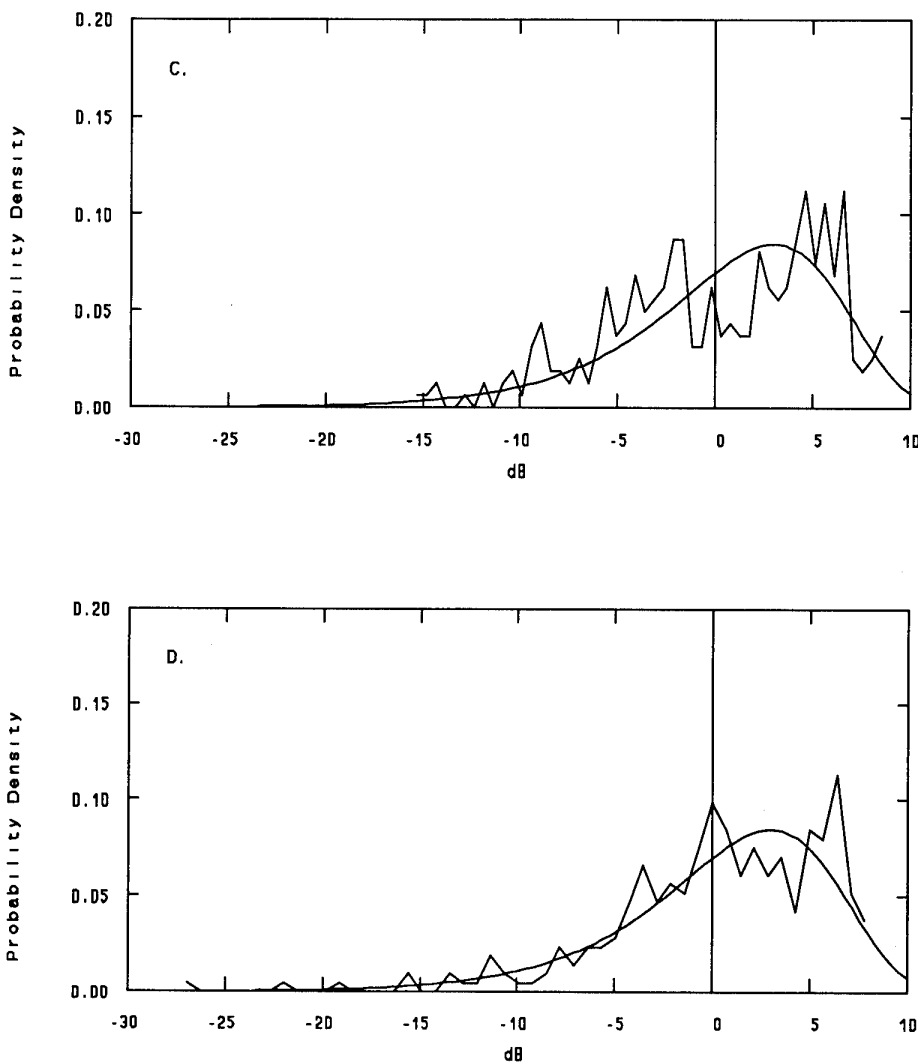


**Figure 8:** Distribution of spatial variation of sound pressure level measured along straight line in MOD Salisbury test tank with source at fixed location (jagged line), compared with theory for Rayleigh distributed rms pressure values (smooth curve): (c) source frequency 4 kHz, (d) 8 kHz

spatially averaged total sound pressure will be 3 dB higher than due to either the direct or the reverberant components, as this distance corresponds with equality of energy densities of each of the two components. At fractions or multiples of the distance  $r_0$ , the relation between the received spatial average of sound pressure level in dB and the true direct or reverberant sound pressure level must be determined.

In order to anticipate the amount of spatial variability existing at the distance  $r_0$ , and at various fractions of it, a Monte Carlo-type simulation was carried out in which the standard deviation  $\sigma$ , in dB, of Rician distributed values was determined for various ratios of constant to random components. At the time

this simulation was carried out, it did not appear that there was any known expression for the required standard deviation. The results of this simulation, including the corresponding fraction of  $r_0$ , the ratio of random to constant power, the randomicity (ratio of random power to total power as used by Urick, for example, reference (7)), and the difference between the total and the direct sound field contributions in dB, are given in Table 3. Here, it is assumed that the values of power are spatial averages. Note that in Table 3, the constant component is labelled "direct" and the random component is labelled "reverberant", so as to correspond with the terminology in the preceding material.

*Table 3: Sound Field Properties at Different Fractions of Reverberation Radius,  $r_0$*

fraction of $r_0$	reverberant: direct power	randomicity	$\sigma$ dB	total - constant power, dB
$> r_0$	1:0	1.0000	5.57	no constant power
$r_0$	1:1	0.5000	4.92	3.00
$r_0/2$	1:4	0.2000	2.99	0.97
$r_0/3$	1:9	0.1000	2.02	0.46
$r_0/4$	1:16	0.0588	1.50	0.26
$r_0/5$	1:25	0.0385	1.20	0.17

Clearly, the closer the measurement position to the sound source, the smaller the spatial variability. Also, the closer the measurement position to the sound source, the smaller the correction between the mean of the total noise level and the mean of the direct sound field component.

For the purposes of obtaining accurate measurements, taking a single sample of sound pressure at a distance equal to a large fraction of  $r_0$  is impractical, as such a single sample is subject to a large potential error resulting from the high standard deviation shown in the 4th column of Table 3. A practical solution is to take a number of measurements at locations separated by  $\lambda/2$ , this distance, as mentioned earlier, corresponding to independence of mean square pressures for omni-directional receivers in perfectly diffuse fields. In air-filled room acoustics, microphone traverse mechanisms for spatial averaging are possible, however, for a water-filled test tank, this is not feasible - averaging of independent measurements may be the only way to achieve spatial averaging. (It is conceivable, for example, to hold either the source or the receiver in a frame and to move the other vertically in the tank, thereby achieving spatial averaging.)

As Schroeder showed in reference (8) and mentioned in reference (9), for sound levels expressed in dB, in the reverberant field, the standard deviation  $\sigma_{res}$  resulting from averaging along a straight line traverse is approximately given by

$$\sigma_{res} \approx \frac{5.57}{\sqrt{(1 + X/0.3\lambda)}} \text{ dB.} \quad (21)$$

where       $X$     is length of straight line traverse used for receiver, m  
 $\lambda$         is wavelength, m

Schroeder also states that the equivalent number of spatially independent discrete sampling points is equal to the term  $(1 + X/0.3\lambda)$  in equation (21). Thus for  $N_{\text{samp}}$  independent samples of sound pressure level in the reverberant field, equation (21) becomes

$$\sigma_{\text{res}} \approx \frac{5.57}{\sqrt{N_{\text{samp}}}} \text{ dB} . \quad (22)$$

It is tempting to suggest, but not yet proven, that for measurements carried out in regions for which the direct sound field contribution is significant, the resultant standard deviation  $\sigma_{\text{res}}$ , from  $N_{\text{samp}}$  spatially independent samples of sound pressure level in dB, is given by

$$\sigma_{\text{res}} \approx \frac{\sigma}{\sqrt{N_{\text{samp}}}} \text{ dB} . \quad (23)$$

where       $\sigma$     is given by fourth column in Table 3

With no other knowledge, it may be assumed that the spatial separation for sample independence for use of equation (23) is the same as for the fully reverberant field case, that is, a separation distance of  $\lambda/2$  between samples.

## 2.8 Averaging of Spectral Variability

For a fixed source, the rms pressure received at a fixed location in the reverberant field in a highly reverberant chamber, will vary with frequency. The variability is expected to be the same as occurs with changing location at a fixed frequency, that is, the rms pressure values will be Rayleigh distributed. This follows, as the received level is, again, due to the phase coherent combination of a large number of random vectors. Extensive measurements of this phenomenon were taken in the MOD Salisbury test tank, and, while these will be described in a future report, some data will be presented below to illustrate this aspect of the tank's properties and confirm the requirement for spectral averaging.

The spectral variability in the MOD Salisbury test tank was measured using a fixed source and a fixed hydrophone receiver, with a very slowly varying frequency of emission at a constant level of output (SL). Figure 9 shows the frequency response measured from 1400 to 2600 Hz, for a particular set of source and receiver locations.

Each location was at least 2 m from any boundary surface and from the other location. The received signal was sampled using a 16 bit analog to digital converter with a maximum quantisation error on level of 0.003 dB. The curve was produced using an 800 line FFT in a swept sine measurement with a spectral line separation of 1.5625 Hz. Peak Hold (averaging) was employed over the duration of the sweep ( $\approx 15$  mins); the sweep was at a constant rate versus time. Thus the signal was in each filter band for  $\approx 1.125$  seconds. This duration was adequate for stabilisation as it greatly exceeded (by factor of  $\approx 4$ ) the measured reverberation time,  $T_{60}$ , which is a measure of the time for the multiple paths of transmission to sum together. Here we assume the filter

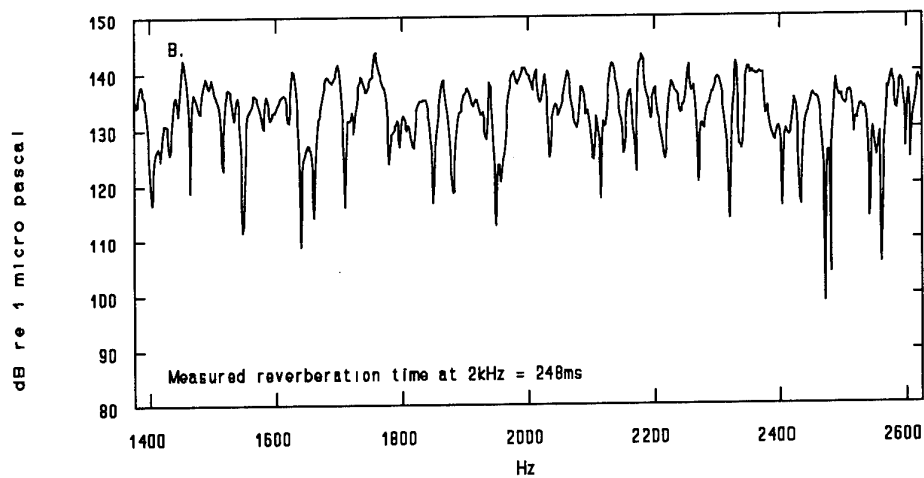


**Figure 9:** Spectral variation of sound pressure measured in MOD Salisbury test tank with source and receiver at fixed locations: swept sine source frequency 1400 - 2600 Hz

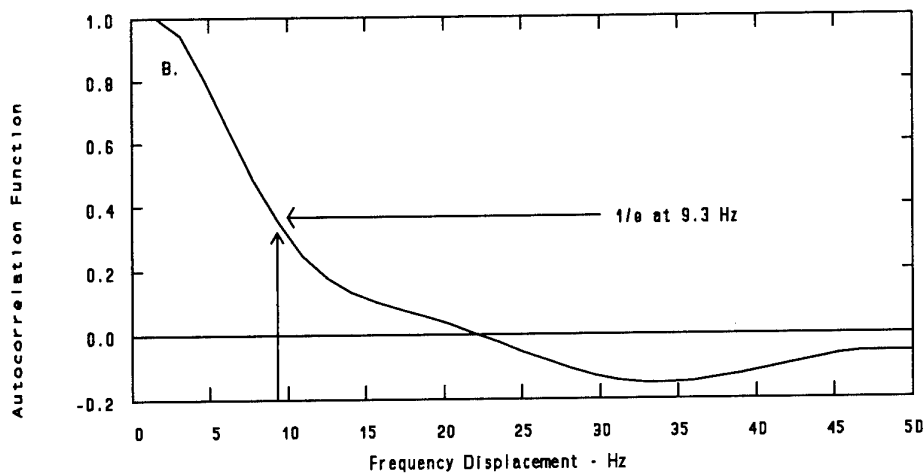


**Figure 10:** Autocorrelation of linear rms sound pressure measured in MOD Salisbury test tank with source and receiver at fixed locations: sine sweep source frequency 1400 - 2600 Hz; for 0 - 50 Hz frequency displacement

bandwidth was be equal to the spectral line separation as a flat weighted time window was used.

Figure 10 shows the normalised estimate of the autocorrelation function obtained using linear, rms pressure data extracted from the curve in Figure 9, with the  $e^{-1}$  point indicated. The curve in Figure 10 is taken to a frequency displacement of 50 Hz.

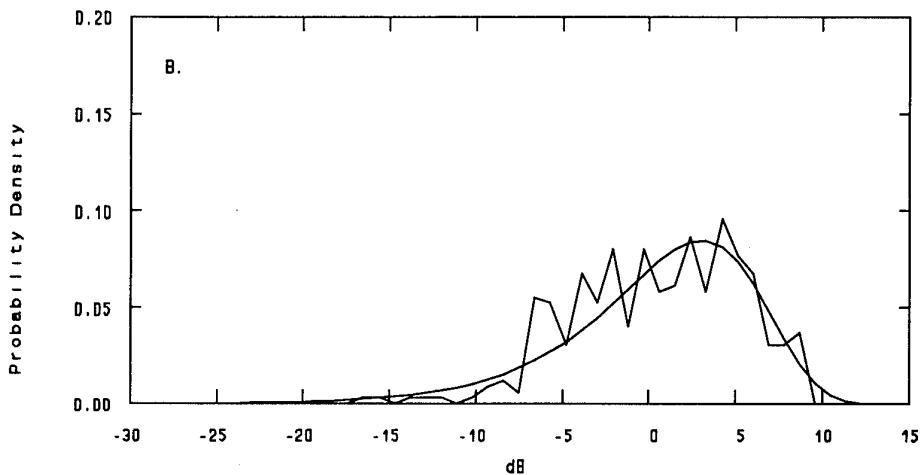


**Figure 11:** Distribution of spectral variation of sound pressure level measured in MOD Salisbury test tank with source and receiver at fixed locations (jagged line), compared with theory for Rayleigh distributed rms pressure values (smooth curve): sine sweep source frequency 1400 - 2600 Hz

Figure 11 shows the associated probability density function (pdf) for sound pressure level, using 50 uniform class intervals over the range -30 to 15 dB about the mean, compared with that for Rayleigh distributed rms values (given by Dyer (reference (5))). The measurement pdf is based on 800 data samples.

The results presented in Figure 9 clearly indicate that spectral variability is a significant phenomenon in the MOD Salisbury test tank. Figure 10 indicates that the frequency response in the tank, in the vicinity of 2 kHz, is significantly de-correlated with a frequency shift of only about 9 Hz. Further, the traces in Figure 11 show that, for the range 1400 - 2600 Hz, the spectral variations of rms pressure are a good fit to the Rayleigh distribution.

In practice, the use of spatial averaging, to arrive at a value of sound pressure level, and thus a value of spatially averaged mean square pressure,  $\overline{p_{rev}^2}$ , for use in equations (17) and (20), may not be as convenient as using averaging across a band of frequencies, should this be possible. From Schroeder (for example, references (8) and (9)), the relation corresponding to equation (21), for averaging the received sound pressure level in dB over a band of frequencies of bandwidth  $W$  is given by

$$\sigma_{res} \approx \frac{5.57}{\sqrt{1 + 0.238 T_{60} W}} \text{ dB.} \quad (24)$$

Here, we may also suggest a similar, but unproven, relation for the standard deviation in dB,  $\sigma_{res}$  of the frequency-averaged received sound pressure level as obtained at locations in the water-filled tank corresponding with the fractions of the reverberation radius  $r_0$ , as indicated in Table 3:

$$\sigma_{res} \approx \frac{\sigma}{\sqrt{1 + 0.238 T_{60} W}} \text{ dB}, \quad (25)$$

where  $\sigma$  is given by fourth column in Table 3

As an example of the effect of spectral averaging, for a reverberation time of 0.15 seconds, which is of the order of the actual value for the MOD Salisbury test tank at some frequencies, averaging over a frequency band of 85 Hz results in the standard deviation of variability, as given by equation (25), being approximately halved. Averaging over 650 Hz results in the standard deviation being reduced by a factor of about 5. For measurements carried out in the reverberant field, this will result in a standard deviation of  $5.57/5 \approx 1.1$  dB.

By comparing equations (24) and (22) and equations (25) and (23), we see that for sound pressure expressed logarithmically, the effect of spectrally averaging

across an additional bandwidth of  $W = \frac{4.20}{T_{60}}$  is equivalent to spatially

averaging across one additional independent sample. Thus, for the MOD Salisbury test tank, assuming a reverberation time of 0.15 seconds, averaging across 85 Hz is equivalent to averaging measurements at 4 positions each at least  $\lambda/2$  apart. Averaging over a bandwidth of 650 Hz is equivalent to averaging at 24 independent positions.

## 2.9 Lower Frequency Limit

As mentioned in section 2.1, there is a lower frequency limit for which a reverberant acoustical chamber, such as the MOD Salisbury test tank, may not be used for either direct field or reverberant field measurements. The reason for this limit is that the chamber alters the radiation impedance acting on a sound source placed in the chamber, from the value applying to free field conditions. A second reason (a direct cause of the first reason) is the breakdown of the assumption of a highly multi-modal chamber, which also occurs at low frequencies.

As shown by Pierce, for example, in reference (2), the average modal density, that is, the average number of modes per unit angular frequency bandwidth,

$\frac{dN}{d\omega}$  is given by

$$\frac{dN}{d\omega} = \frac{1}{2} \frac{V \omega^2}{\pi^2 c^3} = \frac{1}{2\pi (\Delta f)_{mode}}, \quad (26)$$

where  $\omega$  is angular frequency, rad/s  
 $(\Delta f)_{mode}$  is the average spacing between successive room resonance frequencies, in Hz.

From Pierce, for example, the bandwidth of a resonance peak,  $(\Delta f)_{res}$ , defined as the frequency band which encloses the points on the spectrum at which the sound intensity is half the peak value, is given by

$$(\Delta f)_{res} = \frac{1}{2\pi\tau} = \frac{6 \ln 10}{2\pi T_{60}} = \frac{2.20}{T_{60}} \text{ Hz.} \quad (27)$$

When the chamber resonances are spaced more closely than the bandwidth associated with any particular peak, each resonance itself has a less noticeable effect on the frequency response function of the chamber. For average spacing between peaks  $(\Delta f)_{mode}$  being less than  $\frac{1}{3}(\Delta f)_{res}$ , the resonance peaks are assumed (reference (2)) to be smoothed-out. The frequency below which this no longer holds is regarded, somewhat arbitrarily, as the lower frequency limit for the applicability of much of the above room acoustics theory. In honour of M. R. Schroeder, this frequency is known as the Schroeder cutoff frequency,  $f_{Sch}$ , and thus follows as

$$f_{Sch} = \sqrt{\frac{c^3 T_{60}}{4 V \ln 10}} \text{ Hz.} \quad (28)$$

For the dimensions of the MOD Salisbury test tank given in Figures 1 and 2, the chamber volume, being the volume of water in the tank, is approximately  $200 \text{ m}^3$ . For a reverberation time of 0.15 seconds, from equation (28), the Schroeder cutoff frequency, being the lower limiting frequency for the use of the MOD Salisbury test tank as a reverberant chamber, is approximately 510 Hz.

## 2.10 Upper Frequency Limit

The analysis presented above for reverberant chambers is valid so long as the absorption of sound within the chamber is entirely from incidence upon the chamber boundaries. This is perfectly true at low frequencies, but at very high frequencies absorption occurs within the fluid. As shown, for example, in chapter 7 of reference (4) the absorption is dependent upon the square of the frequency and the properties of the fluid. Thus, an upper frequency limit may be specified above which the absorption within the fluid becomes significant. At higher frequencies a chamber may no longer be assumed to be "reverberant" and used as shown above.

From reference (4), the absorption,  $\alpha$ , within a fluid caused by shear and bulk viscosity is given by

$$\alpha = \frac{8 \pi^2 f^2}{3 \rho c^3} \left( \eta + \frac{3}{4} \eta_B \right). \quad (29)$$

- where     $\alpha$     is pressure amplitude absorption coefficient, nepers/m (at  $\frac{1}{\alpha}$  m distance, the pressure amplitude has dropped to  $\frac{1}{e}$  of its initial value)  
 $f$     is frequency, Hz  
 $\eta$     is coefficient of shear viscosity, Pa · s  
 $\eta_B$     is coefficient of bulk viscosity, Pa · s

Note that equation (29) is relevant for fresh water, but not for sea water, for which additional absorption mechanisms exist (e.g. reference (4)).

A more convenient measure of absorption is  $a$ , the spatial rate of decrease in intensity level expressed as dB/m. As shown, for example, in section 7.2 of reference (4),  $a = 20(\log_{10} e)\alpha \approx 8.69\alpha$ . Thus we have

$$a \approx \frac{229 f^2}{\rho c^3} \left( \eta + \frac{3}{4} \eta_B \right). \quad (30)$$

where  $a$  is intensity absorption coefficient, dB/m

This absorption per unit distance,  $a$ , may now be used to compare the absorption occurring within the fluid to the absorption provided by the boundary surfaces of the chamber. Here, the link is the reverberation time,  $T_{60}$ , as shown below.

In a reverberant chamber, the permissible amount of absorption within the fluid may be specified as some proportion of the total absorption. For example, one may specify the maximum desired fluid absorption,  $x$  dB, which may occur within the time for the boundary surfaces to provide 60 dB absorption. But, by definition, 60 dB absorption is provided by the boundary surfaces in the time known as the reverberation time,  $T_{60}$ . Further,  $T_{60}$  is the time for sound to travel  $c T_{60}$  metres. Thus,  $a \times c T_{60}$  dB absorption occurs within the fluid in the time that the boundary surfaces provide 60 dB absorption. By substituting for  $a$  from equation (30), we then have the maximum desired fluid absorption  $x$  dB. By re-arranging terms, we may arrive at the following frequency requirement for a fluid absorption of less than  $x$  dB within the reverberation time  $T_{60}$  for a chamber:

$$f < \sqrt{\frac{\rho c^2 x}{229 T_{60} \left( \eta + \frac{3}{4} \eta_B \right)}} \quad (31)$$

where  $x$  is maximum permissible absorption within the fluid, dB

For the MOD Salisbury test tank, for a maximum fluid absorption of 1 dB within the reverberation time (assumed to be 0.15 seconds), using values of density, sound velocity and shear viscosity for fresh water of  $998 \text{ kg/m}^3$ ,  $1481 \text{ m/s}$  and  $0.001 \text{ Pa} \cdot \text{s}$ , respectively (appendix 10 reference (4)), and assuming that the bulk viscosity is 2.81 times the shear viscosity (e.g. reference (10)), the maximum frequency for the use of the chamber is 143 kHz.

### 3. Measurements and Estimation of Acoustical Properties of MOD Salisbury Test Tank

The following sections present the results of investigations of the acoustical properties of the MOD Salisbury test tank, determined by both measurements and estimations. The purpose of this work was to study the acoustical properties of the MOD Salisbury test tank with reference to the theoretical descriptions of section 2. In particular, it was considered desirable to study the relationship between the measured reverberation time and the reflective nature of the chamber boundary surfaces. This was done, as the theoretical description of the chamber properties in section 2 showed that all dependent properties are related to the chamber reverberation time. A further purpose of

this work was to see how accurately the reverberation time, and hence chamber properties might be estimated from a description of the structural features of the chamber and its boundaries.

The estimation of the absorptive properties of the MOD test tank was preceded by measurements of the sound reflective properties of the concrete walls of the tank. The effect of these properties on the taking of accurate measurements in the tank is considered.

### **3.1 Water-Wall Pressure Amplitude Reflection Coefficient Measurements**

The normal incidence pressure amplitude reflection coefficient of the tank wall (water to concrete interface),  $R_{wall}$ , was measured at the following frequencies: 1000, 2000, 4000 and 8000 Hz. The method used was one that relied on measuring the amplitude of a tone burst both before and after normal incidence upon a section of the tank wall. By accounting for the spreading losses of the reflected pulse due to the geometry of the tank, the pressure reflection coefficient was determined, based on the total observed decrease in pulse intensity.

It must be stated that these measurements were carried out in the assumption that the tank walls were locally reactive, rather than modally reactive. In other words, it was assumed that an incident plane wave was reflected as a plane wave, rather than being diffracted upon reflection. Also, in later determinations of the average chamber sound power absorption coefficient, it was assumed that the pressure amplitude reflection coefficient was not dependent upon the angle of incidence.

#### **3.1.1 using the elliptical geometry of the tank**

The technique involved generating a tone burst which propagated past a hydrophone, continued onto the tank wall and was reflected back to the hydrophone. The normal incidence pressure amplitude reflection coefficient  $R_{wall}$  was determined by comparing the amplitude of the signal before reflection  $P_{direct}$  to that of the reflected signal  $P_{reflect}$  measured at the hydrophone. The resultant amplitude ratio had to be normalised to account for the spreading loss of the signal. The spreading loss was, in turn, dependant on the directivity of the acoustic projector used and the geometry of the tank wall. For this work, specular reflection of the sound was assumed.

For these tests, as shown in Figures 1 and 2, the acoustic projector was located at one of the focal points of the ellipse, as viewed from above, and near mid-depth in the tank. The directivity of the projector was assumed to be spherical. Thus the tone burst emitted by the projector was assumed to spread spherically until the tank wall was reached. As the tank wall is flat when viewed in the vertical plane, from this view-point the radiation appeared to continue to spread spherically after reflection, as shown in Figure 1. However, when viewed in the horizontal plane, as the projector was located at one of the focal points of the ellipse, all ray paths were reflected back to the second focal point, as shown in Figure 2. The result of this geometrical arrangement was for the pulse to spread spherically until incidence with the tank wall, and for

the reflection from the wall to focus to a vertical line at the second focal point of the ellipse. For measurement purposes, a hydrophone was placed so that it received a direct signal (tone burst) followed by the return signal, as shown in Figure 12.

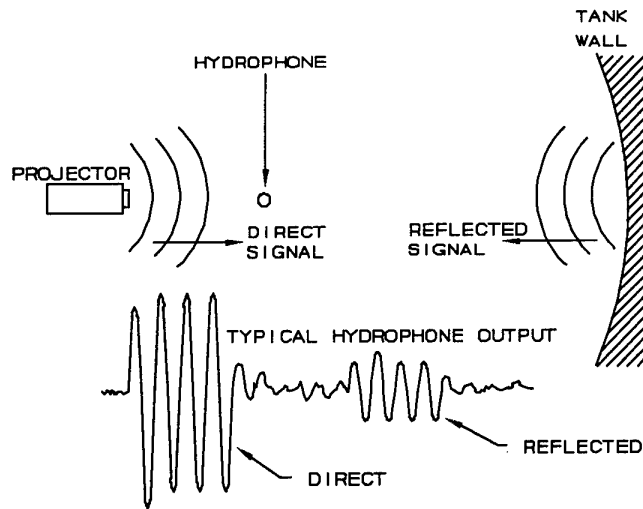


*Figure 12: Experimental Setup in Plan View & Typical Output Signal, MOD Salisbury Test Tank*

The amplitude ratio  $\frac{P_{direct}}{P_{reflect}}$  expected at the hydrophone position for a normal incidence pressure amplitude reflection coefficient of 1.0 was predicted as follows:

The incident, or direct, signal spread spherically until it reached the wall whereupon, in the vertical plane it continued as if spreading spherically, whilst in the horizontal plane it converged to F2 (refer Figure 2). During the initial spherical spreading stage, the sound intensity decreased in inverse proportion to the square of the distance from the projector and the pressure amplitude decreased in inverse proportion to the distance from the projector. However, following the reflection, the spreading relationship changed and was no longer simply spherical, due to the convergence as viewed from the horizontal plane.

As shown in Figure 13, the sound intensity of the signal before and after reflection from the tank walls may be depicted as being proportional to the area bounded by acoustic ray paths. For spherical spreading, the dimensions are proportional to the distance from the projector. At any point along the ray paths, the acoustic pressure amplitude is proportional to the square-root of the area enclosed by the rays.

Figure 13 portrays the direct signal intensity as it passed the hydrophone at a distance of 200 mm by the small square. This square has dimensions  $200x$  mm  $\times$   $200x$  mm, where  $x$  is a constant of proportionality. At the wall, the same sound energy was projected onto a larger area, with dimensions  $1500x$  mm  $\times$   $1500x$  mm. On reflection, the signal continued spreading in the

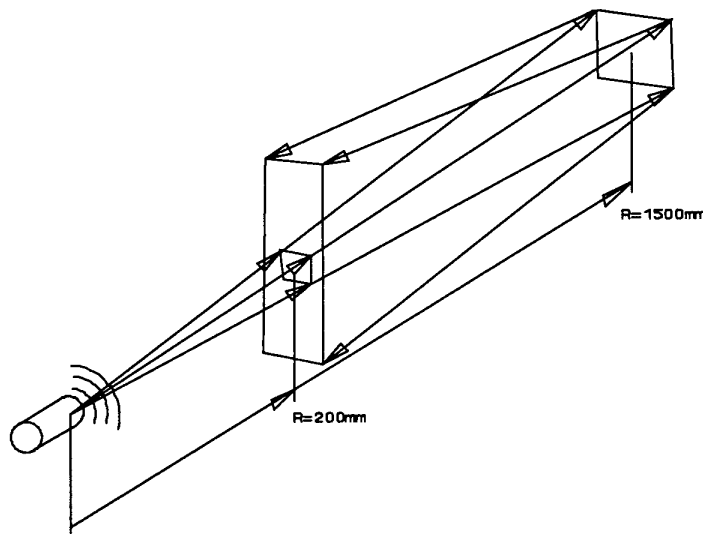


**Figure 13:** Sound Intensity Area Ratios

vertical plane in proportion to the total distance travelled from the source. Thus the vertical separation of the reflected rays at the hydrophone position was  $1500x + 1300x = 2800x$  mm. In the horizontal plane, the reflected signal converged to the second focal point of the ellipse and hence the horizontal ray separation was a function of the distance from the hydrophone to location F2 and the distance from the wall to location F2 - that is, the horizontal dimension was  $1500x \times (4700/6000) = 1175x$  mm (refer Figure 2).

Thus the pressure amplitude ratio measured at the hydrophone, for a pressure amplitude reflection coefficient of 1.0 follows as:

direct signal area at the hydrophone =  $0.2x \times 0.2x$ ,

$$\therefore P_{\text{direct}} \sim \sqrt{\text{Area}} = 0.2x \text{ m},$$

reflected signal area at the hydrophone =  $2.800x \times 1.175x$ ,

$$\therefore P_{\text{reflect}} \sim \sqrt{\text{Area}} = 1.8138x \text{ m},$$

$\therefore$  pressure amplitude ratio for a reflection coefficient of 1.0 follows as

$$\frac{P_{\text{direct}}}{P_{\text{reflect}}} = \frac{1.8138}{0.2} \approx 9.07.$$

### 3.1.2 reflection coefficient measurements

The pressure amplitude ratio of the direct and reflected signals at the hydrophone was measured, so that the pressure amplitude reflection coefficient of the water to wall interface might be determined. For example, a pressure amplitude ratio of 11.27 for a 4 kHz tone of one cycle duration was measured, as shown in Figure 14. For two reasons, a pulse of one cycle, only, was used

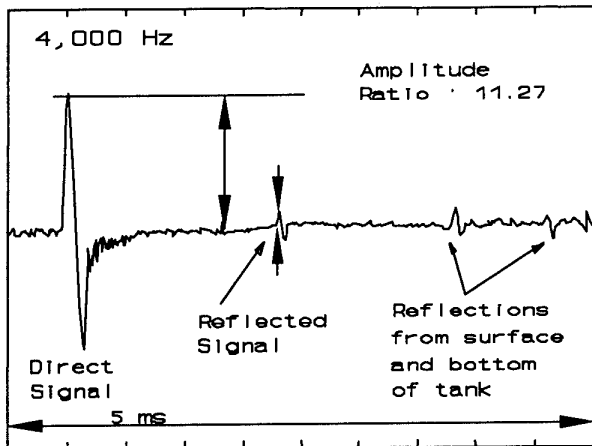


*Figure 14: Hydrophone Output At 4kHz, MOD Salisbury Test Tank*

at each of the frequencies, to limit the signal duration: firstly, this ensured separation of the wall reflection from the surface and bottom reflections at lower frequencies for which longer pulse durations applied; secondly, as the geometry of the tank walls might not necessarily be as perfect as indicated by Figures 1 and 2, there was some chance of irregular reflections combining in incorrect phase relation. In performing the measurements, no distortion effects were observed to be caused by the projector transients.

The normal incidence pressure amplitude reflection coefficient,  $R_{wall}$ , was found as described above. For example:

measured normal incidence pressure amplitude reflection coefficient at

$$4 \text{ kHz} = \frac{9.07}{11.27} \approx 0.80.$$

Table 4 shows the values of normal incidence pressure amplitude reflection coefficient for each of the frequencies investigated. No attempt has been made to check the variation of these measurements with the time of year. It might be expected that the ground properties, and thus the acoustic reflective properties of the tank wall, may be dependent upon the recent history of rainfall.

*Table 4: Measurements of Normal Incidence Pressure Amplitude Reflection Coefficient,  $R_{wall}$ , MOD Salisbury Test Tank*

Frequency	1000 Hz	2000 Hz	4000 Hz	8000 Hz
$R_{wall}$	0.66	0.73	0.80	0.79

### 3.2 Water-Air Pressure Amplitude Reflection Coefficient Estimation

The MOD Salisbury test tank has, of course, a large part of its surface area

existing as a water-air interface, at the water surface. Whilst a normal incidence pressure amplitude reflection coefficient near to -1.0 may be assumed for this surface, it was considered desirable to determine this value with more precision.

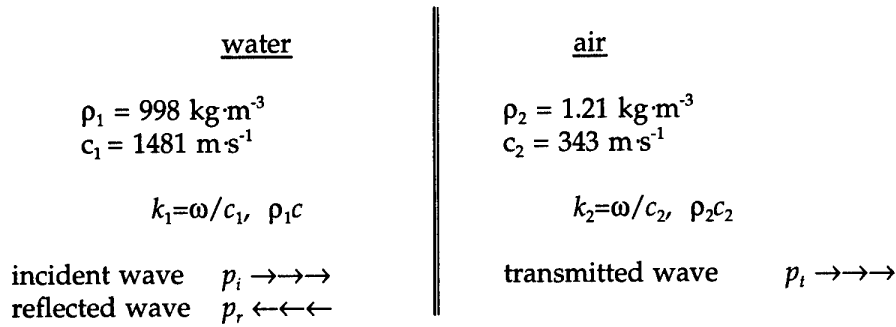


**Figure 15:** Water - Air Interface

Consider the boundary shown in Figure 15 (appendix 10, reference (4)). Here, the instantaneous acoustic particle velocities,  $u$ , and pressures,  $p$ , at angular frequency  $\omega$ , may be expressed in terms of incident, reflected and transmitted waves of pressure amplitude  $A_1$ ,  $B_1$  and  $A_2$  respectively (for example, see reference (4) section 6.2) as:

$$u_i = \frac{p_i}{\rho_1 c_1}, \quad p_i = A_1 e^{j(\omega t - k_1 x)} \quad (32)$$

$$u_r = - \frac{p_r}{\rho_1 c_1}, \quad p_r = B_1 e^{j(\omega t + k_1 x)} \quad (33)$$

$$u_t = \frac{p_t}{\rho_2 c_2}, \quad p_t = A_2 e^{j(\omega t - k_2 x)} \quad (34)$$

At the interface, there is continuity of pressure:

$$p_i + p_r = p_t \text{ at the boundary } (x = 0), \quad \therefore A_1 + B_1 = A_2.$$

At the interface, there is continuity of particle velocity:

$$\begin{aligned} u_i + u_r &= u_t \text{ at the boundary } (x = 0), \\ \therefore \frac{A_1 - B_1}{\rho_1 c_1} &= \frac{A_2}{\rho_2 c_2} \Rightarrow \frac{A_1 - B_1}{\rho_1 c_1} = \frac{A_1 + B_1}{\rho_2 c_2}. \end{aligned} \quad (35)$$

Resolving for  $B_1$  and  $A_1$  ...

$$\Rightarrow \frac{B_1}{A_1} = \frac{\rho_2 c_2 - \rho_1 c_1}{\rho_2 c_2 + \rho_1 c_1}. \quad (36)$$

where  $B_1/A_1$  is the required pressure amplitude reflection coefficient,  $R_{air}$ .

For the water to air interface in this experiment, this results in a pressure amplitude reflection coefficient  $R_{air}$  of -0.9994 for normal incidence at the surface.

### 3.3 Estimation of Tank Sound Power Absorption Coefficient

In order to determine the sound power (or  $SL$ ) of a sound source using either the direct field method, with equation (16) (and (18)), or the reverberant field method with equation (17) (and (20)), an estimate must be made of the overall sound absorption coefficient for the water-filled test tank,  $\bar{\alpha}$ . Once the normal incidence pressure amplitude reflection coefficient for each particular different boundary surface of the test tank is known, the term  $\bar{\alpha}$  may be evaluated using equation (7). Then the reverberation time  $T_{60}$  may be found using equation (8), the radius of reverberation  $r_0$  from equation (14), the room constant  $R_{rc}$  from equation (11) and hence the sound power may be determined.

For the MOD Salisbury test tank, the weighted average sound power absorption coefficient  $\bar{\alpha}$  is thus calculated using the water to wall and the water to air sound power absorption coefficients  $\alpha_{wall}$  and  $\alpha_{air}$ , respectively, by weighting these values according to their associated tank surface areas. These values, in turn, may be obtained directly from the measured pressure amplitude reflection coefficient values, as:

$\beta_{wall} = |R_{wall}|^2$ ,  $\beta_{air} = |R_{air}|^2$ , where the sound power reflection coefficients  $\beta_{wall}$  and  $\beta_{air}$  are proportional to the square of the pressure amplitude coefficients (for example, reference (4), section 6.1). Assuming  $\beta_{wall} + \alpha_{wall} = 1$ ,  $\beta_{air} + \alpha_{air} = 1$ , (energy balance at the interface), the sound power absorption coefficients  $\alpha_{wall}$  and  $\alpha_{air}$  may be found directly.

The sound power absorption coefficient for the water to wall interface is thus obtained from the values of normal incidence pressure amplitude reflection coefficient from Table 4, and is shown in Table 5.

*Table 5: Wall Reflection and Absorption Coefficients, MOD Salisbury Test Tank*

Frequency	pressure amplitude reflection coefficient $R_{wall}$	sound power reflection coefficient $\beta_{wall}$	sound power absorption coefficient $\alpha_{wall}$
1000 Hz	0.66	0.44	0.56
2000 Hz	0.73	0.53	0.47
4000 Hz	0.80	0.64	0.36
8000 Hz	0.79	0.62	0.38

The sound power absorption coefficient at the water to air interface,  $\alpha_{air}$ , follows from the calculated pressure amplitude reflection coefficient  $R_{air}$  determined in section 3.2. This value is therefore:

$$\alpha_{air} = 1 - (-0.9994)^2 = 0.0012.$$

Now, the weighted average absorption coefficient,  $\bar{\alpha}$ , is given by equation (7), reproduced here for clarity:

$$\bar{\alpha} = \frac{\sum_i \alpha_i A_i}{A} ,$$

where  $A_1$  = area of water to wall interface for tank  $\approx 160 \text{ m}^2$ ,  $A_2$  = area of water to air interface for tank  $\approx 35.3 \text{ m}^2$ ,  $\alpha_1 = \alpha_{wall}$  values given in Table 5,  $\alpha_2 = \alpha_{air}$ , and  $A = A_1 + A_2 \approx 195 \text{ m}^2$ .

For the MOD Salisbury test tank, the estimated average sound power absorption coefficient for each of the frequencies considered is thus given in Table 6.

**Table 6: Estimated Average Sound Absorption Coefficients for MOD Salisbury Test Tank**

Frequency	1000 Hz	2000 Hz	4000 Hz	8000 Hz
$\bar{\alpha}$	0.46	0.39	0.30	0.31

The values of average sound power absorption shown in Table 6 correspond with a rating of either "dead" or "medium-dead" according to Figure 9.4 of reference (1). Measurements of both spatial and spectral variability carried out in the MOD Salisbury test tank, do, however, indicate that this chamber has sufficiently reverberant characteristics to be used for measurement purposes. That is, at measurement distances greater than the reverberation radius, the pressure amplitude was shown to follow the Rayleigh distribution.

### 3.4 Estimated Reverberation Times

The reverberation time is defined here as the time required for the ensemble sound energy density within the tank to decay 60 dB from its original value, after the sound source has been turned off at  $t = 0$  seconds. This decay time is given by equation (8), reproduced here for clarity:

$$T_{60} = \frac{0.0373 V}{\sum_i \alpha_i A_i} ,$$

where  $V$  is volume of water in tank  $\approx 200 \text{ m}^3$ .

For the MOD Salisbury test tank, the values of reverberation time estimated using this procedure, whilst using the values of sound absorption and area for the wall and air interface segments indicated in section 3.3, are as shown in Table 7.

**Table 7: Estimated Reverberation Times for MOD Salisbury Test Tank,  $T_{60}$  (ms)**

Frequency	1000 Hz	2000 Hz	4000 Hz	8000 Hz
$T_{60}$ ms	83	99	129	123

### 3.5 Measured Reverberation Times

The reverberation time  $T_{60}$  was measured by abruptly stopping the output from a sound projector and recording the decay of acoustic pressure with a hydrophone placed at least  $\frac{1}{4}\lambda$  from any surface (e.g. section 6.4 of reference (1)). A sample of such a measurement of the instantaneous pressure decay recorded for a pure tone of 1 kHz is shown in Figure 16. Here, the tank was insonified for 400 ms before sampling began, after which the projector was stopped at  $t = 0$  seconds. The decay shown in Figure 16 indicates the presence of many chamber modes and the associated phase cancelling causing the amplitude modulation.

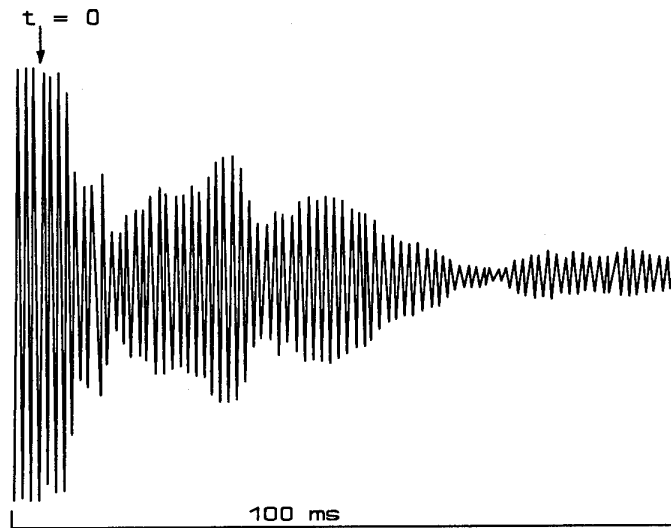


**Figure 16:** Reverberant decay of instantaneous pressure at fixed receiver in MOD Salisbury Test Tank @ 1 kHz

Ideally, one desires a decay curve giving the average acoustic energy density or the volume average of squared pressure versus time following source switch-off. This volume average can be approximated by the running time averages of many hydrophones spaced for independence (at least  $\lambda/2$  apart) throughout the tank. However, the test equipment was limited to only one receiver, and so several decays were recorded digitally at different times and locations within the tank whilst maintaining the same source position and output settings. These recordings of instantaneous pressure were then squared and averaged. To reduce the erratic nature of the decay curves, the data was integrated in time using the following integral (reference (11)):

$$10 \log_{10} \left( \frac{1}{T_{ref}} \int_t^{\infty} \frac{p^2(t)}{p_{ref}^2} dt \right) \quad (37)$$

where  $T_{ref}$  is any arbitrarily chosen constant

This function is more representative of the decay of the total sound energy in the tank because the deviations of  $p^2(t)$  from its long term trend are not viewed

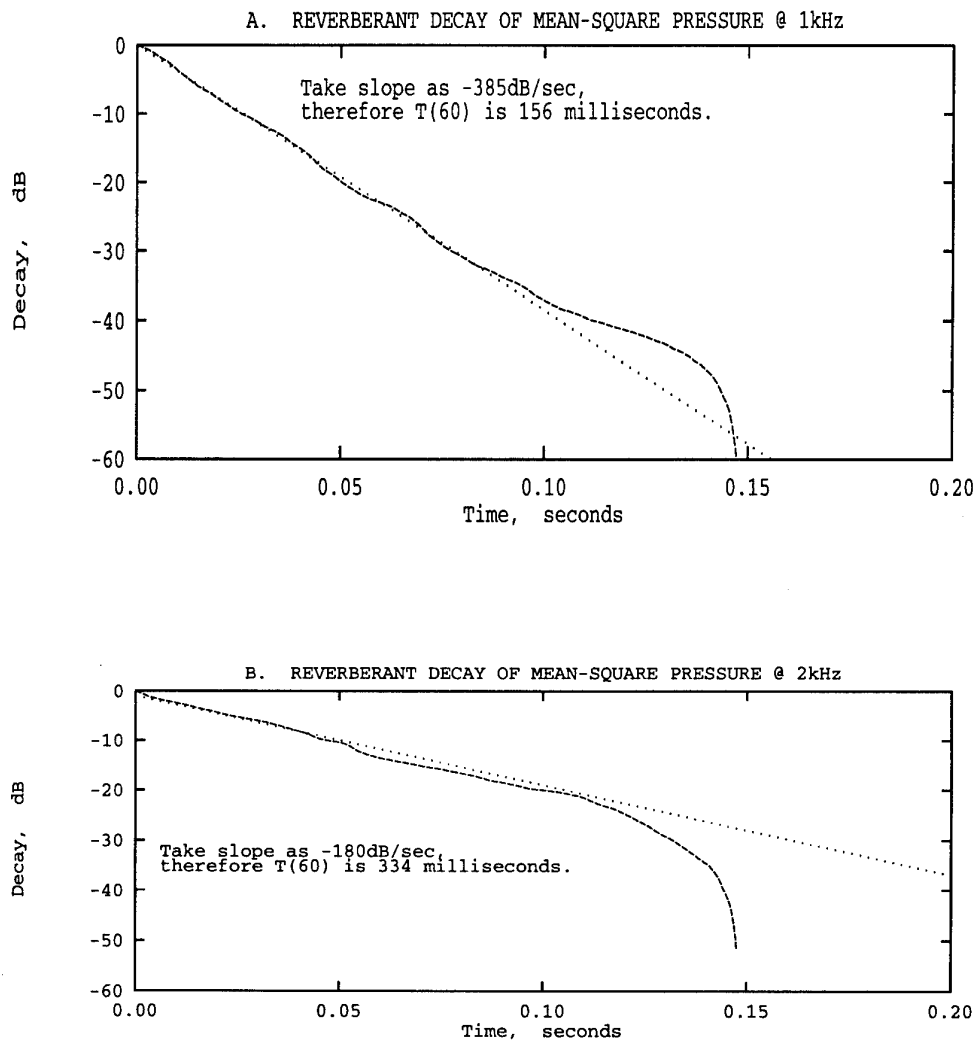


**Figure 17:** MOD Salisbury test tank reverberant decay curves integrated in time: (a) at source frequency 1 kHz, (b) 2 kHz. The measured decay curves are depicted by dashed lines. The dotted lines are an estimate of a uniform decay rate for use in the analysis.

in isolation and have the appearance of being averaged out over the duration of the decay. The slope of this curve gives the decay rate in decibels per second and is equal to  $60/T_{60}$ . Figures 17 and 18 show the curves from equation (37) at each frequency, using five recordings of instantaneous pressure to obtain an average decay curve before integrating. Here, the tank was insonified with pure tone signal for a period not less than two seconds before source switch-off. (Note that the trace shown in Figure 16 was not from the same particular series of measurements.)

The data for Figures 17 and 18 was acquired at the rate of 125,000 samples per second over a period of 160 milliseconds, which is also the period over which

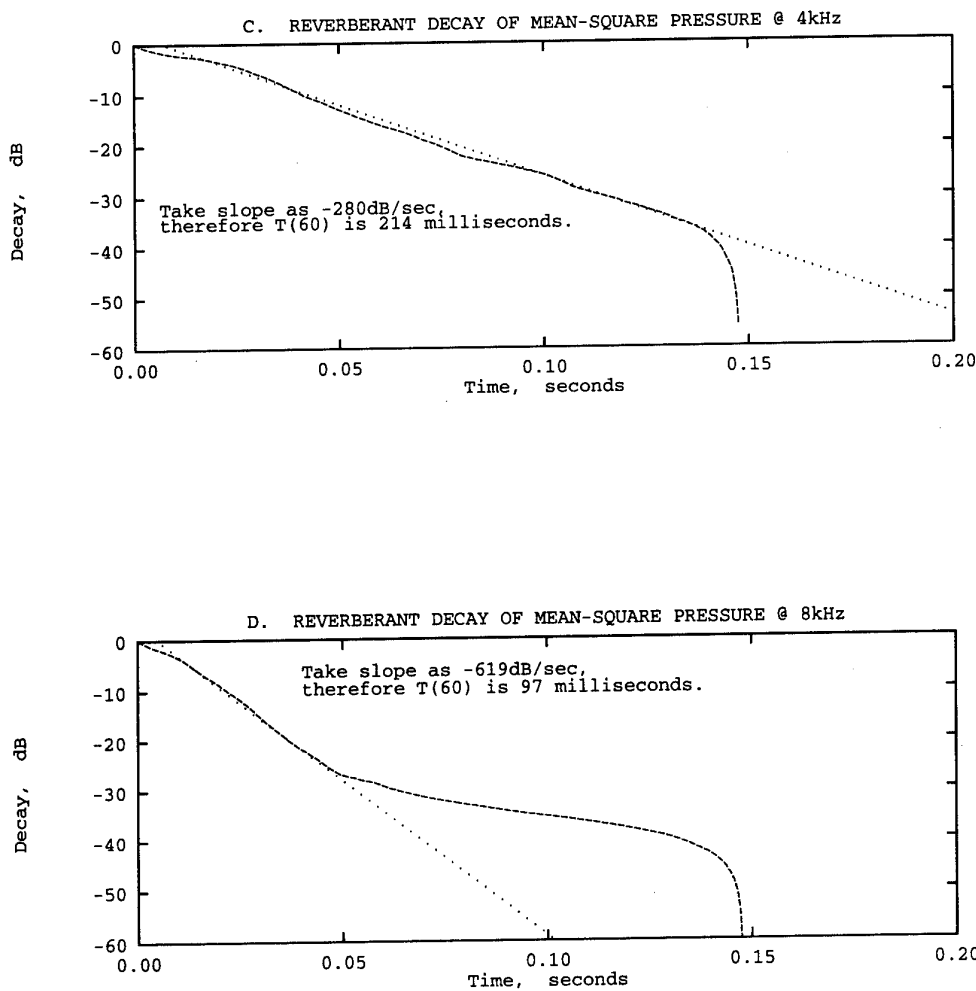


**Figure 18:** MOD Salisbury test tank reverberant decay curves integrated in time: (c) at source frequency 4 kHz, (d) 8 kHz. The measured decay curves are depicted by dashed lines. The dotted lines are an estimate of a uniform decay rate for use in the analysis.

equation (37) was integrated. As the sound pressure level did not decay to zero over this integration period due to the ambient noise floor, all the curves in Figures 17 and 18 exhibit a drooping tail which is characteristic of equation (37) being treated as a finite integral. In Figure 18 (d), the reverberant sound at 8 kHz quickly decayed into the noise floor. Thus the curve appears to be composed of two slopes. The reverberation time obtained using this procedure, for each of the frequencies studied, is shown in Table 8, together with the respective estimated value taken from Table 7.

**Table 8: Measured & Estimated Reverberation Times,  $T_{60}$ , for MOD Salisbury Test Tank (ms)**

Frequency	1000 Hz	2000 Hz	4000 Hz	8000 Hz
Estimated $T_{60}$	83	99	129	123
Measured $T_{60}$	156	334	214	97

Clearly, from Table 8, the values of reverberation time estimated from the assumed normal incidence pressure amplitude reflection coefficients are of the order of those measured directly, whilst not being identical.

In practice, the measurement of reverberation time may be facilitated by the use of spectral averaging, as this may achieve the same result as spatial averaging, as described in section 2.8. A single hydrophone at a fixed location may thus be used in such a measurement procedure. Knowledge of the bandwidth over which the averaging must occur does, of course, need the reverberation time as an input. In practice, once the order of magnitude of the reverberation time is known from an initial pure tone-based measurement, the required bandwidth  $W$  which gives the desired averaging may be found from equation (24). Using the procedure described in section 2.8, it may be shown that spectrally averaging across a bandwidth of about 110 Hz is equivalent to spatially averaging the reverberation decay curves at 5 independent positions, for a reverberation time of 0.15 seconds.

Measurements of the reverberation time must, of course, be made in the reverberant field of the test chamber, that is, at greater distances from the insonifying source than the radius of reverberation,  $r_0$ . Again, the determination of this distance is dependent upon the knowledge of the reverberation time,  $T_{60}$ , as shown by equation (15). Some trial and error may thus be required before the extent of the reverberant field is known. In measurements of reverberation time, the sound projector must function for a duration at least several times the reverberation time, to ensure full insonification. This follows from the complementary nature of sound build-up and decay in a reverberant chamber, which has been shown to exist by Schroeder in reference (12).

### 3.6 Reverberation Radius Determined from Measurements

If the MOD Salisbury test tank is to be used as a means of determining the sound power of acoustic sources, then the distance from a sound source at which the energy density from the direct field becomes equal to, and ultimately less than, that of the reverberant field must be known. Direct field measurements of sound pressure may then be taken within this distance, known as the reverberation radius  $r_0$ , this being determined by equations (14) or (15) in section 2.4. Alternatively, reverberant field measurements may be taken at greater distances from the source than  $r_0$ .

Now, using the measured values for the reverberation time listed in Table 8, the effective average sound power absorption coefficient,  $\alpha_e$ , may be determined using a re-arranged version of the Sabine equation, equation (8), as follows:

$$\alpha_e = \frac{0.0373 V}{T_{60} A} \quad (38)$$

where  $\alpha_e$  is effective absorption coefficient derived from measured reverberation times

$V$  is volume of water in tank,  $200 \text{ m}^3$

$A$  is total surface area of tank boundaries,  $195 \text{ m}^2$

The value of  $\alpha_e$  was determined using equation (38) for each of the frequencies studied, using the measured reverberation time from Table 8 as input. Each derived values is shown in Table 9, together with the respective estimated value  $\bar{\alpha}$  taken from Table 6.

**Table 9: Effective & Estimated Sound Absorption Coefficients for MOD Salisbury Test Tank**

Frequency	1000 Hz	2000 Hz	4000 Hz	8000 Hz
estimated $\bar{\alpha}$	0.46	0.39	0.30	0.31
effective $\alpha_e$	0.25	0.12	0.18	0.41

Clearly, the effective values shown in Table 9 are smaller than the estimated values, at all but the highest frequency. The MOD Salisbury test tank was thus more highly reverberant than expected at frequencies up to 4000 Hz. At 8000 Hz, the tank was found to be less reverberant than expected. The effective values of average sound power absorption,  $\alpha_e$ , shown in Table 9 correspond with the following ratings, according to Figure 9.4 of reference (1): "medium-dead" (1000 Hz), "medium-live to average" (2000 Hz), "average to medium-dead" (4000 Hz), "dead" (8000 Hz).

In room acoustics, when the term  $\alpha_e$  is determined from measurements, it is the usual practice (for example, reference (2)) for the room constant to be simplified as  $R_{rc} = \alpha_e A$ , due to the expectation of errors in measurement and a consequent lack of precision. Using equation (8), and substituting  $\alpha_e A$  in place of  $\sum_i \alpha_i A_i$ , we arrive at the following expression for the reverberation radius, based on equation (14) (note the similarity with the more precise equation (15)):

$$r_0 = \sqrt{\frac{0.0373 V Q_\theta}{16 \pi T_{60}}} \quad (39)$$

Table 10 lists the reverberation radius values obtained using the measured reverberation times of Table 8 in equation (39), and shows the values obtained with the more precise equation (15). Note that these values of reverberation radius have been determined for an omnidirectional sound source, for which  $Q_\theta$  has the value 1.0.

**Table 10:** Reverberation Radius,  $r_0$ , Based on Measured Reverberation Time, MOD Salisbury Test Tank (for omnidirectional sound sources)

Frequency	1000 Hz	2000 Hz	4000 Hz	8000 Hz
$r_0$ (metres), from equation (39)	0.98	0.67	0.83	1.24
$r_0$ (metres), from precise equation (15)	1.12	0.71	0.92	1.59

From the values shown in Table 10, the reverberation radius determined by the approximate method, equation (39), is not greatly different to that obtained with the more precise equation (15). In general, equation (39) underestimates the value. Clearly, based on this determination of reverberation radius, measurements of the sound pressure emitted by a source may be obtained in the direct field dominated region of the MOD Salisbury test tank at most frequencies of interest. A problem arises if a source dimension is larger than this distance, or if the reverberation radius is within the zone near the source for which near field interference effects occur. For point sources, such as a piston-type projector, this will not be a problem. For piston sources, it is true that measurements within the reverberation radius, for some frequencies, may be within the zone near the source for which the sound pressure is not in phase with the particle velocity. This is often, mistakenly, considered to be a region in which sound pressure measurements for the determination of the sound power of the source may not be made, however, in this region the sound pressure from the direct field varies linearly in proportion to the reciprocal of the distance from the source, right up to the vibrating surface of the source in the case of a spherical radiator, and so measurements may, in fact, be taken.

In practice, if equation (16) is used to determine the sound power of a source by taking measurements in the direct field, some kind of spatial or frequency averaging, as described in sections 2.5.1 and 2.5.2, respectively, may be necessary. Also, the relevant power correction factor, listed in the fifth column of Table 3 must be applied.

### 3.7 Effect of Changing Absorption of Tank Walls

#### 3.7.1 increasing absorption

The MOD Salisbury test tank currently has sound absorption properties which are inherent to the nature of its construction. However, there is some potential to improve the direct field measuring capability of the tank if the averaged sound absorption of its boundary surfaces was increased.

If the averaged sound power absorption coefficient of the boundaries of the tank,  $\bar{\alpha}$ , was doubled, from the Sabine equation, equation (8), the reverberation time  $T_{60}$  would then be halved, from equation (10) the room constant  $R_{rc}$  would be approximately doubled and from equation (12) the reverberation radius  $r_0$  would increase by  $\sqrt{2}$ . Thus the distance from a sound source at which the direct field contribution was greater than the reverberant field contribution

would be increased by  $\sqrt{2}$  and direct field measurements taken in the tank may become more convenient to perform.

As is well known, some water-filled acoustical test tanks are lined in particular anechoic materials. If such a lining was applied to the walls of the MOD Salisbury test tank, and  $\bar{\alpha}$  was doubled, it might be expected that the reverberation radii, as shown in Table 9, might be increased by, the order of  $\sqrt{2}$ . A further advantage of increased sound absorption is the resultant decrease in the frequency,  $f_{Sch}$ , at which measurements may be carried out in the tank. From equation (28), the Schroeder cutoff frequency will decrease by a factor of  $\sqrt{2}$  (to about 360 Hz) if the reverberation time is halved.

### 3.7.2 *decreasing absorption*

A water test tank constructed as an above-ground facility, with relatively thin walls of wooden, concrete or metal construction, is likely to have good sound reflection from the above-ground walls, as these walls will present a low acoustic impedance. This, combined with high sound reflection from the air-water interface, will give rise to a long reverberation time,  $T_{60}$ , and a small reverberation radius,  $r_0$ . This, in turn, will enable reverberant field measurements to be carried out more easily, as hydrophones may then be placed more closely to a source. However, equation (28) shows that an increase in reverberation time gives rise to an increase in the Schroeder cutoff frequency,  $f_{Sch}$ , this rising in proportion to the square root of the reverberation time.

## 4. *Procedures for Measurements*

The previous sections of this report describe the development of the relevant theory, and the conduct of the necessary measurements, by which the MOD Salisbury test tank has been characterised as an acoustical measurement facility. For the benefit of those who wish to use this facility, or any other water-filled test tank, the important conclusions of the earlier sections of this report are summarised below, in the form of a practical user guide. For the purposes of brevity and clarity, this user guide has been prepared so that it may be read in isolation from the remainder of the report. No reference is made to the earlier sections which contain the relevant derivations, however, the inquisitive reader will have no difficulty in finding this material and may be assured that the detail is all included above.

### 4.1 *SL and Sound Power Measurements*

In general, underwater sound sources and receivers which are usually operated in free space should be located near to the centre of the chamber, to ensure that the chamber boundary surfaces do not have a reaction on the source (or receiver).

#### 4.1.1 direct sound field

An acoustic receiver<sup>3</sup> will be in the direct sound field of a source in a water-filled test tank if the source to receiver separation is much less than the radius of reverberation,  $r_0$ , given by

$$r_0 = \sqrt{\frac{0.0373 V Q_\theta}{16\pi (T_{60} - 0.0373 V/A)}}$$

- where  $V$  is volume of water in tank, m<sup>3</sup>  
 $Q_\theta$  is directivity of sound source, non-dimensional.  $10 \log_{10} Q_\theta$  is the same as the directivity index,  $DI$ , of the sound source  
 $T_{60}$  is reverberation time (time for acoustic energy density to decay 60 dB), seconds  
 $A$  is total surface area of tank boundaries, m<sup>2</sup>

For a receiver located in the direct sound field of a sound source in a test tank filled with fresh water, the source level,  $SL$ , defined as the (maximum) axial response as an rms sound pressure in dB extrapolated to a position 1 m from the acoustical centre of the source, may be determined by measurement as

$$SL = SPL_{dir} + 20 \log_{10} r \text{ dB re 1 m.}$$

- where  $SPL_{dir}$  is rms sound pressure level at distance  $r$  due to direct field, dB re 1  $\mu$ Pa  
 $r$  is distance from source, m

The corresponding sound power output of the sound source in watts,  $P$ , may be determined by measurement as

$$P = \frac{10^{\left(\frac{SPL_{dir}}{10}\right)} r^2}{1.17 \times 10^{17} Q_\theta} \text{ watts.}$$

The  $SL$  may be determined from a measurement of the direct field sound pressure level,  $SPL_{dir}$ , taken at any distance from a monopole source existing as a pulsating sphere. Such a measurement may even be taken at a point on the surface of the sphere, regardless of the acoustic wavelength (so long as the displacement of the surface is much less than the radius of the sphere). For a piston radiator, a measurement may be taken at a minimum distance of about two diameters from the centre of the piston.

Dependent upon the ratio of the measurement distance from the acoustical centre of a sound source to the radius of reverberation, a value of  $SPL_{dir}$  may need to be obtained from a measurement procedure which includes either spatial or spectral averaging, or both. In such a case, a correction term,  $SPL_{corr}$ , must be subtracted from the measured sound pressure level,  $SPL_{meas}$ , to obtain the value of  $SPL_{dir}$ . The required value of this correction term is shown in the

---

<sup>3</sup> For this section, it is assumed that the receiver has omnidirectional sensitivity to sound pressure.

table below:

*Direct Field Measurement at Different Fractions of Reverberation Radius,  $r_0$*

distance from sound source as fraction of $r_0$	correction term $SPL_{corr}$ dB $(SPL_{dir} = SPL_{meas} - SPL_{corr})$
$> r_0$	no direct field contribution
$r_0$	3.00
$r_0/2$	0.97
$r_0/3$	0.46
$r_0/4$	0.26
$r_0/5$	0.17

#### 4.1.2 reverberant sound field

An acoustic receiver will be in the reverberant sound field in a water-filled test tank if the source to receiver separation is greater than the radius of reverberation,  $r_0$ . For a receiver in the reverberant sound field, the  $SL$  may be determined by measurement as

$$SL = SPL_{rev} + 10 \log_{10} V + 10 \log_{10} Q_0 - 10 \log_{10} \left( T_{60} - \frac{0.0373V}{A} \right) - 31.3 \text{ dB.}$$

where  $SPL_{rev}$  is sound pressure level of spatially averaged rms sound pressure due to reverberant field, dB re 1  $\mu\text{Pa}$

The corresponding sound power output of the sound source in watts,  $P$ , may be determined by measurement as

$$P = \frac{10^{\left(\frac{SPL_{rev}}{10}\right)} V}{1.58 \times 10^{20} \left( T_{60} - \frac{0.0373V}{A} \right)} \text{ watts.}$$

A value of  $SPL_{rev}$  must be obtained from a measurement procedure which includes either spatial or spectral averaging, or both. Dependent upon the ratio of the measurement distance from the acoustical centre of the sound source to the radius of reverberation, a correction term,  $SPL_{corr}$ , must be subtracted from the measured sound pressure level,  $SPL_{meas}$ , to obtain the value of  $SPL_{rev}$ . The required value of this correction term is shown in the table below:

*Reverberant Field Measurement at Different Fractions of Reverberation Radius,  $r_0$*

distance from sound source as multiple of $r_0$	correction term $SPL_{corr}$ dB $(SPL_{rev} = SPL_{meas} - SPL_{corr})$
$r_0$	3.00
$2r_0$	0.97
$3r_0$	0.46
$4r_0$	0.26
$5r_0$	0.17
$> r_0$	0.00

Measurements of sound pressure in the reverberant field must be taken in areas of the chamber in which the sound field may be regarded as diffuse. Some rules of thumb, largely from section 6.4 of reference (1), are as follows:

- (a) No hydrophone measurement should be made less than one major source dimension from the source, even if the reverberation radius is smaller than this dimension.
- (b) For highly directional sources, hydrophone measurements should not be taken in the line of source direction
- (c) No hydrophone should be placed more closely to a chamber boundary surface than  $\frac{\lambda}{4}$  at the frequency of interest.

## 4.2 Directivity Measurements

### 4.2.1 source directivity

Once the  $SL$ , defined as the axial response (that is, along the axis with the maximum response), has been determined from a direct field measurement<sup>4</sup>, as described in section 4.1.1, the directivity of the source may be determined using a corresponding measurement of the rms sound pressure level in the reverberant field,  $SPL_{rev}$ . The directivity of the source,  $Q_0$ , is non-dimensional. It is more convenient to deal with the directivity index,  $DI$ , of the source, which is the same as  $10 \log_{10} Q_0$  (see, for example, page 184 of reference (4)). The directivity index may then be determined as

$$DI = SL - SPL_{rev} - 10 \log_{10} V + 10 \log_{10} \left( T_{60} - \frac{0.0373 V}{A} \right) + 31.3 \text{ dB.}$$

A more direct method, requires the use of a second source which is known to be omni-directional. Here, the known source is substituted for the unknown,

---

<sup>4</sup> For this section, it is assumed that the receiver has omnidirectional sensitivity to sound pressure.

after the on-axis output from each, as determined by a receiver in the close direct field, has been adjusted to be the same. Corresponding measurements of the rms sound pressure level in the reverberant field,  $SPL_{rev}$ , are then used to determine the  $DI$ . Here, the reduction in the reverberant field dB level that occurs when the unknown source insonifies the chamber is the same as its  $DI$ .

#### **4.2.2 receiver directivity**

If an omnidirectional sound source is used, the directivity of a receiver may be determined. Here the  $SL$  must be measured by the subject receiver in a direct field measurement as described in section 4.1.1, with the receiver axis of maximum response directed at the source. The directivity index of the receiver may then be determined using a corresponding measurement of the rms sound pressure level in the reverberant field,  $SPL_{rev}$ , as

$$DI = SL - SPL_{rev} - 10 \log_{10} V + 10 \log_{10} \left( T_{60} - \frac{0.0373V}{A} \right) + 31.3 \text{ dB.}$$

A more direct method, requires the use of a second receiver which is known to be omni-directional. Here, both receivers are placed in the close direct field of the omni-directional source and, by finding the axis of maximum response for the unknown receiver, the on-axis output of each receiver is adjusted to be the same. Corresponding measurements of the rms sound pressure level recorded by each receiver in the reverberant field ( $SPL_{rev}$ ) are then used to determine the  $DI$  of the unknown receiver. Here, the reduction in the dB level received by the unknown receiver is the same as its  $DI$ .

### **4.3 Spatial Averaging**

Unless the distance of a receiver from the sound source is much less than the radius of reverberation,  $r_0$ , the received signal is highly variable with position in a test tank and spatial or spectral averaging, or both, must be employed. Also, for all but large multiples or small fractions of distance  $r_0$  from the sound source, the averaged sound pressure will be composed of significant direct and reverberant components, and procedures described in sections 4.1.1 and 4.1.2 must be used to determine either component based on a measurement.

The spatially-averaged amount of spatial variability existing at the distance  $r_0$ , and at various fractions of it, is expressed as a standard deviation,  $\sigma$ , in dB in the table below.

*Spatial Variability at Different Fractions of Reverberation Radius,  $r_0$*

fraction of $r_0$	standard deviation of variability $\sigma$ dB
$> r_0$	5.57
$r_0$	4.92
$r_0/2$	2.99
$r_0/3$	2.02
$r_0/4$	1.50
$r_0/5$	1.20

Clearly, the closer the measurement position to the sound source, the smaller the spatial variability. For larger distances, the spatial variability may be reduced by either averaging measurements along a straight line traverse, or averaging a number of (spatially independent) measurements taken at locations separated by at least  $\lambda/2$ .

For sound levels expressed in dB, the standard deviation  $\sigma_{res}$  resulting from averaging along a straight line traverse is approximately given by

$$\sigma_{res} \approx \frac{\sigma}{\sqrt{(1 + X/0.3\lambda)}} \text{ dB.}$$

where       $\sigma$     is standard deviation of variability from table above, dB  
                $X$     is length of straight line traverse used for receiver, m  
                $\lambda$     is wavelength, m

The standard deviation  $\sigma_{res}$  resulting from averaging  $N_{samp}$  (independent) measurements at fixed locations separated by at least  $\lambda/2$  is given by

$$\sigma_{res} = \frac{\sigma}{\sqrt{N_{samp}}} \text{ dB.}$$

where       $\sigma$     is standard deviation of variability from table above, dB

#### 4.4 Spectral Averaging

The variability of received sound pressure level, as measured in a water-filled test tank, is the same for a fixed geometry and changing frequency as it is for a fixed frequency and changing location, for a given fraction of the distance  $r_0$  from the sound source. Spectral averaging may thus be employed to reduce the variability in measured sound pressure levels, in dB. Also, for all but large multiples or small fractions of distance  $r_0$  from the sound source, the averaged sound pressure will be composed of significant direct and reverberant components, and procedures described in sections 4.1.1 and 4.1.2 must be used to determine either component based on a measurement.

For sound levels expressed in dB, the standard deviation  $\sigma_{res}$  resulting from averaging the received sound pressure level in dB over a band of frequencies of bandwidth  $W$  is given by

$$\sigma_{res} \approx \frac{\sigma}{\sqrt{1 + 0.238 T_{60} W}} \text{ dB},$$

where  $\sigma$  is standard deviation of variability from table in section 4.3 above, dB

#### 4.5 Lower Limiting Frequency

Measurements of the characteristics of underwater sound sources and receivers may be carried out in a water-filled test tank at frequencies above the Schroeder cutoff frequency,  $f_{Sch}$ , given by

$$f_{Sch} = \sqrt{\frac{c^3 T_{60}}{4 V \ln 10}} \text{ Hz.}$$

where  $c$  is the sound velocity, m/s  
 $T_{60}$  is reverberation time (time for acoustic energy density to decay 60 dB), seconds  
 $V$  is volume of water in tank,  $\text{m}^3$

For the MOD Salisbury test tank, based on a measured reverberation time at 1000 Hz of about 0.15 seconds, a water volume of  $200 \text{ m}^3$ , and the speed of sound in fresh water of 1481 m/s, the Schroeder cutoff frequency is about 510 Hz.

#### 4.6 Upper Limiting Frequency

Measurements of the characteristics of underwater sound sources and receivers may be carried out in a water-filled test tank at frequencies up to that for which sound absorption within the water becomes significant.

For a fluid with absorption caused by shear and bulk viscosity, the frequency  $f_{max}$ , for which the absorption within the fluid is less than  $x$  dB in a period within the reverberation time for a chamber, is given by

$$f_{max} = \sqrt{\frac{\rho c^2 x}{229 T_{60} \left( \eta + \frac{3}{4} \eta_B \right)}}.$$

where  $f_{max}$  is frequency, Hz  
 $x$  is maximum permissible absorption within the fluid, dB  
 $\eta$  is coefficient of shear viscosity,  $\text{Pa} \cdot \text{s}$   
 $\eta_B$  is coefficient of bulk viscosity,  $\text{Pa} \cdot \text{s}$

For the MOD Salisbury test tank, for a maximum fluid absorption of 1 dB within the reverberation time of about 0.15 seconds, based on values of density, sound velocity and shear viscosity for fresh water of  $998 \text{ kg/m}^3$ , 1481 m/s and  $0.001 \text{ Pa} \cdot \text{s}$ , respectively, and assuming that the bulk viscosity is 2.81 times the shear viscosity, the maximum frequency for the use of the chamber is 143 kHz.

## 4.7 Measurements of Reverberation Time

The reverberation time is the time required for the ensemble sound energy density within a chamber to decay 60 dB from its original value, after a sound source, which has fully insonified the chamber, has been turned off instantaneously. The reverberation time for a chamber should be evaluated shortly before other measurements are carried out. Chambers such as the MOD Salisbury test tank, which have water-ground interfaces, may be affected by soil moisture content and so the value of  $T_{60}$  may be dependent upon recent weather events, as well as the time of year.

The reverberation time may be measured by fully insonifying the chamber and then abruptly stopping the output from the sound projector whilst continually recording the decay of acoustic pressure with a hydrophone placed at least  $\lambda/4$  from any surface. To ensure full insonification, the sound projector must function for a duration at least several times the reverberation time.

The desired decay curve is one which gives the average acoustic energy density or the volume average of squared pressure versus time following source switch-off. This volume average can be approximated by the running time averages of many hydrophones spaced for independence (at least  $\lambda/2$  apart), however it is usually more convenient to achieve this result with spectral averaging of the output from a single hydrophone. The resultant instantaneous pressure is then squared and, in the case of several measurements, averaged. To reduce the erratic nature of the decay curves, the data may be integrated in time as follows:

$$10 \log_{10} \left( \frac{1}{T_{ref}} \int_t^\infty \frac{p^2(t)}{p_{ref}^2} dt \right)$$

where  $T_{ref}$  is any arbitrarily chosen constant  
 $p_{ref}$  is reference acoustic pressure, 1  $\mu\text{Pa}$  (20  $\mu\text{Pa}$  for air acoustics)

The slope of this curve gives the decay rate in decibels per second and is equal to  $60/T_{60}$ . Values of the reverberation time which have been obtained for the MOD Salisbury test tank using this procedure, based on pure tone insonification and spatial averaging, are shown in the table below.

*Measured Reverberation Times,  $T_{60}$ , for MOD Salisbury Test Tank (ms)*

Frequency	1000 Hz	2000 Hz	4000 Hz	8000 Hz
Measured $T_{60}$	156	334	214	97

If spectral averaging is employed in the measurement of reverberation time, an averaged decay on a single hydrophone at a fixed location in the chamber is adequate. The spectral averaging achieved by using a bandwidth  $W$  is equivalent to spatially averaging at  $1 + 0.238 T_{60} W$  independent positions (each  $\lambda/2$  apart). Knowledge of the bandwidth over which the averaging is effective thus needs the reverberation time as an input. Thus, once the order of magnitude of the reverberation time is known from an initial pure tone-based measurement, the required bandwidth  $W$  which gives the desired averaging may be found. If averaging equivalent to that achieved by using 5

independent positions is desired, then the required bandwidth  $W = \frac{16.8}{T_{60}}$ .

Measurements of the reverberation time must be made in the reverberant field of the test chamber, that is, at greater distances from the insonifying source than the radius of reverberation,  $r_0$ . Again, the determination of this distance is dependent upon the prior knowledge of the reverberation time,  $T_{60}$ . Some trial and error may thus be required before the extent of the reverberant field is known.

## 5. *Conclusions*

The MOD Salisbury test tank has been shown to have a perfectly diffuse sound field at frequencies above approximately 510 Hz. This facility is thus suitable to be used for acoustical measurements requiring either a reverberant or a direct sound field above about 510 Hz. For such higher frequencies, the chamber does not impose any back-reaction upon a sound source, and, depending upon source directivity and size, sound sources in the MOD Salisbury test tank will operate exactly as they will in an ocean environment of infinite extent. Note that sound absorption within the water in the chamber imposes a maximum frequency for testing of about 150 kHz.

The acoustical properties of the MOD Salisbury test tank have been measured and are in very good agreement with expectations based on existing room acoustic theory. The reverberation radius, being the distance from a sound source within which the direct sound field dominates the reverberant sound field, was determined for several frequencies and was found to be convenient for the taking of sound pressure measurements in either the direct or reverberant fields. Generally speaking, the reverberation radius is about 1 m. In terms of the descriptions used for acoustical chambers, the MOD Salisbury test tank has the following ratings: "medium-dead" (1000 Hz), "medium-live to average" (2000 Hz), "average to medium-dead" (4000 Hz), "dead" (8000 Hz).

If the MOD Salisbury test tank is to be used for reverberant field measurements, or for measurements in all but close proximity to a source, either spatial averaging or spectral averaging techniques, will be necessary. To enhance the use of the test tank for sound power measurements, the absorptive properties of the tank walls must be increased by adding an absorptive lining to the walls.

A knowledge of the reverberation time,  $T_{60}$ , is essential to the use of this or any other reverberant chamber for  $SL$ , sound power and, depending on technique, source or receiver directivity measurements. The reverberation time is related to all dependent acoustical properties of an acoustical chamber. It is required for specifying the reverberation radius, the lower frequency limit for measurements in the chamber, and for determining the bandwidth over which spectral averaging must be performed. For the MOD Salisbury test tank, the reverberation time was of the order of 0.2 seconds, and was frequency dependent.

A reasonably accurate estimation of the reverberation time of the MOD Salisbury test tank was made, on the basis of the tank construction details, and a sample measurement of the normal incidence pressure amplitude reflection coefficient of the tank wall. It is thus expected that the properties of other reverberant chambers may be estimated, to a first order accuracy, on a basis of their physical properties, dimensions, and properties of the fluid used as the acoustical medium.

## *References*

1. Beranek, L.L. (editor) "Noise and Vibration Control" McGraw-Hill, 1971
2. Pierce, A.D. "Acoustics - An Introduction to Its Physical Principles and Applications" McGraw-Hill, 1981
3. Vanselow, G. "Cost-effective Estimate of Subsea Component Noise Levels" Proceedings of IEEE "Oceans 91" Conference, October 1-3, 1991, Honolulu, Hawaii, pp 1028-1031
4. Kinsler, L.E.; Frey, A.R.; Coppens, A.B. and Sanders, J.V. "Fundamentals of Acoustics", Third edition John Wiley & Sons, 1982
5. Dyer, I "Statistics of Sound Propagation in the Ocean", Journal of the Acoustical Society of America, Vol. 48, No.1 (Part 2), 1970, pp 337-345
6. Blachman, N.M. "Noise and its Effect on Communication", Second Edition, Robert E. Krieger, 1982
7. Urick, R.J. "Models for the amplitude fluctuations of narrow-band signals and noise in the sea", Journal of the Acoustical Society of America, Vol. 62, No. 4, October 1977, pp 878-887
8. Schroeder, M.R. "Effect of Frequency and Space Averaging on the Transmission Responses of Multimode Media", Journal of the Acoustical Society of America, Vol. 46, No. 2 (Part 1), 1969, pp 277-283
9. Schroeder, M.R. "Spatial Averaging in a Diffuse Sound Field and the Equivalent Number of Independent Measurements", Journal of the Acoustical Society of America, Vol. 46, No. 3 (Part 1), 1969, pp 534
10. Urick, Robert J. "Principles of Underwater Sound", 3rd Edition, McGraw-Hill, Inc., 1983
11. Schroeder, M.R. "New Method of Measuring Reverberation Time", Journal of the Acoustical Society of America, Vol. 37, 1965, pp 409-412

12. Schroeder, M.R. "Complementarity of Sound Buildup and Decay", Journal of the Acoustical Society of America, Vol. 40, No. 3, 1966, pp 549-551

---

SECURITY CLASSIFICATION OF THIS PAGE

UNCLASSIFIED

---

REPORT NO.  
DSTO-RR-0068

AR NO.  
AR-009-476

REPORT SECURITY CLASSIFICATION  
UNCLASSIFIED

---

TITLE

Acoustical Properties of the MOD Salisbury Test Tank and Techniques for Measurements

---

AUTHOR(S)  
A.D.Jones and S.A.Hoefs

CORPORATE AUTHOR  
DSTO Aeronautical and Maritime Research Laboratory  
GPO Box 4331  
Melbourne Victoria 3001

---

REPORT DATE  
January, 1996

TASK NO.  
DST 93/023

---

FILE NO.  
510/207/0444

REFERENCES  
12

PAGES  
57

---

CLASSIFICATION/LIMITATION REVIEW DATE

CLASSIFICATION/RELEASE AUTHORITY  
Chief, Maritime Operations Division

---

SECONDARY DISTRIBUTION

Approved for public release

---

ANNOUNCEMENT

Announcement of this report is unlimited

---

KEYWORDS

Reverberant Chamber  
Acoustical Testing

Reverberation Time  
Spatial Variability

Spectral Variability  
Reflection Coefficient

---

ABSTRACT

The acoustical properties of the MOD test tank at DSTO Salisbury were determined, so that the limitations on its use for precise acoustical measurements might be known. The tank properties were measured according to the characterisation usually applied to air-filled reverberant chambers. The measurement of these properties is described, together with a summary of relevant sections of reverberant chamber theory, as re-applied to a water-filled tank. Techniques for using the tank for determining the acoustical power output and directivity of sound sources are described, from both a theoretical and a practical viewpoint. Particular attention is given to the complicating effects of spatial and spectral variability, and a description is given of the means of accounting for these effects. Methods for improving the tank properties are discussed.

---

SECURITY CLASSIFICATION OF THIS PAGE

UNCLASSIFIED

# Acoustical Properties of the MOD Salisbury Test Tank and Techniques for Measurements

A.D.Jones and S.A.Hoefs

(DSTO-RR-0068)

## Distribution List

### AUSTRALIA

#### DEFENCE ORGANISATION

##### Defence Science and Technology Organisation

Chief Defence Scientist }  
FAS Science Policy } shared copy  
AS Science Corporate Management }  
Counsellor Defence Science, London (Doc Data Sheet only)  
Counsellor Defence Science, Washington  
Scientific Adviser to Thailand MRD (Doc Data Sheet only)  
Scientific Adviser to the DRC (Kuala Lumpur) (Doc Data Sheet only)  
Senior Defence Scientific Adviser/Scientific Adviser Policy and Command (shared copy)  
Navy Scientific Adviser (3 copies Doc Data Sheet and one copy of the distribution list)  
Scientific Adviser - Army (Doc Data Sheet and distribution list only)  
Air Force Scientific Adviser  
Director Trials

##### Aeronautical and Maritime Research Laboratory

Director  
Chief, Maritime Operations Division  
Chief, Ship Structures and Materials Division  
Research Leader, Sonar Technology & Processing, MOD  
Research Leader, Submarine and Ship Sonar, MOD  
Research Leader, Mine Warfare, MOD  
Authors: A.D.Jones, MOD Salisbury  
S.A.Hoefs, MOD Stirling  
Mr. S.Taylor, MOD Salisbury  
Dr. D.Liebing, MOD Salisbury  
Dr. J.Riley, MOD Salisbury  
Mr. T.Trainor, MOD Salisbury  
Mr. I.Cox, MOD Salisbury  
Mr. R.Alksne, MOD Salisbury  
Dr. G.Furnell, MOD Salisbury  
Dr. D.McMahon, MOD Salisbury  
Dr. A.Larsson, MOD Salisbury  
Mr. M.Steed, MOD Salisbury  
Dr. B.Jessup, MOD Sydney  
Dr. D.Cato, MOD Sydney  
Dr. B.Ferguson, MOD Sydney  
Mr.F.May, MOD Maribyrnong  
Dr. R.McLeary, MOD Maribyrnong  
Dr. D.Oldfield, SSMD Maribyrnong  
Dr. C.Norwood, SSMD Maribyrnong

(DSTO-RR-0068)

**Distribution List (Contd)**

Mr. R.Juniper, SSMD Maribyrnong

DSTO Library

Library Fishermens Bend  
Library Maribyrnong  
Library DSTOS (2 copies)  
Library, MOD, Pyrmont (2 copies)

Defence Central

OIC TRS, Defence Central Library  
Officer in Charge, Document Exchange Centre (DEC), 11 copies  
Defence Intelligence Organisation  
Library, Defence Signals Directorate (Doc Data Sheet only)

Air Force

Director General Force Development (Air), (Doc Data Sheet only)

Army

Director General Force Development (Land), (Doc Data Sheet only)  
ABC4 Office, G-1-34, Russell Offices, Canberra (4 copies)

Navy

Director General Force Development (Sea), (Doc Data Sheet only)  
SO (Science), Director of Naval Warfare, Maritime Headquarters Annex, Garden  
Island, NSW 2000. (Doc Data Sheet only)  
CO AJAAC, HMAS Albatross, Nowra, NSW  
DOM, MHQ Annex Level 2, Potts Point, NSW  
SOAVN, MHQ Annex, Potts Point, NSW

**UNIVERSITIES AND COLLEGES**

Australian Defence Force Academy  
Library  
Head of Aerospace and Mechanical Engineering  
Deakin University, Serials Section (M list)), Deakin University Library, Geelong, 3217  
Senior Librarian, Hargrave Library, Monash University  
Serials section, Central Library, Flinders University of South Australia

(DSTO-RR-0068)

**Distribution List (Contd)**

**OTHER ORGANISATIONS**

NASA (Canberra)

AGPS

State Library of South Australia

Parliamentary Library, South Australia

Mr. Ian Whitehouse, Nautronix Ltd., 108 Marine Terrace, Fremantle, W.A. 6160

Dr. Louis Raillon, Thomson Sintra Pacific Pty. Ltd., P.O.Box 326, North Ryde, NSW 2113

**ABSTRACTING AND INFORMATION ORGANISATIONS**

INSPEC: Acquisitions Section Institution of Electrical Engineers

Library, Chemical Abstracts Reference Service

Engineering Societies Library, US

American Society for Metals

Documents Librarian, The Center for Research Libraries, US

**INFORMATION EXCHANGE AGREEMENT PARTNERS**

Acquisitions Unit, Science Reference and Information Service, UK

Library - Exchange Desk, National Institute of Standards and Technology, US

Miss M.J.Erith, DRA Farnborough, GU14 6TD, UK

Mr. Roger Pinnington, ISVR, University of Southampton, Southampton, S09 5NH, UK

Dr. Robert W. Timme, Naval Research Lab., P.O.Box 8337, Orlando, Florida, USA

Mr. David M. Deveau, Naval Undersea Warfare Centre, Newport, Rhode Island 02841, USA

Dr. John S. Kay, Defence Scientific Establishment, Auckland Naval Base, Auckland, New Zealand

Prof. Rodney Coates, Electronic and Electrical Engineering, University of Birmingham,

Birmingham, B15 2TT, UK

**SPARES (Normally 10 copies)**